



**HAL**  
open science

# Insights on the particle-attached riverine archaeal community shifts linked to seasons and to multipollution during a Mediterranean extreme storm event

Mégane Noyer, Maria Bernard, Olivier Verneau, Carmen Palacios

## ► To cite this version:

Mégane Noyer, Maria Bernard, Olivier Verneau, Carmen Palacios. Insights on the particle-attached riverine archaeal community shifts linked to seasons and to multipollution during a Mediterranean extreme storm event. *Environmental Science and Pollution Research*, 2023, 10.1007/s11356-023-25637-x . hal-04028116

**HAL Id: hal-04028116**

**<https://hal.inrae.fr/hal-04028116>**

Submitted on 10 Apr 2023

**HAL** is a multi-disciplinary open access archive for the deposit and dissemination of scientific research documents, whether they are published or not. The documents may come from teaching and research institutions in France or abroad, or from public or private research centers.

L'archive ouverte pluridisciplinaire **HAL**, est destinée au dépôt et à la diffusion de documents scientifiques de niveau recherche, publiés ou non, émanant des établissements d'enseignement et de recherche français ou étrangers, des laboratoires publics ou privés.



Distributed under a Creative Commons Attribution 4.0 International License

[Click here to view linked References](#)

1 **Insights on the particle-attached riverine archaeome at different**  
2 **seasons and in response to multipollution during a Mediterranean**  
3 **extreme storm event**

4 Mégane Noyer<sup>1,2</sup>, Maria Bernard<sup>3,4</sup>, Olivier Verneau<sup>1,2,5</sup>, Carmen Palacios<sup>1,2,\*</sup>

5 <sup>1</sup>Univ. Perpignan Via Domitia, CEFREM, UMR5110, F-66860, Perpignan, France.

6 <sup>2</sup>CNRS, CEFREM, UMR5110, F-66860, Perpignan, France.

7 <sup>3</sup>Univ. Paris-Saclay, INRAE, AgroParisTech, GABI, 78350, Jouy-en-Josas, France.

8 <sup>4</sup>INRAE, SIGENAE, 78350, Jouy-en-Josas, France.

9 <sup>5</sup>Unit. for Environmental Sciences and Management, North-West University, ZA-2520,  
10 Potchefstroom, South Africa.

11 **\*Corresponding author:** Carmen Palacios; [carmen.palacios@univ-perp.fr](mailto:carmen.palacios@univ-perp.fr). Centre de  
12 Formation et de Recherche sur les Environnements Méditerranéens UMR 5110 CNRS-UPVD  
13 Université de Perpignan Via Domitia 52 Avenue Paul Alduy 66860 Perpignan Cedex, France.  
14 Phone: + 33468661791. Fax: + 33468662096.

15

16 **Acknowledgments**

17 We would like to thank Cristiana Cravo-Laureau for her suggestions on an advance version of  
18 this manuscript. We are thankful to B. Reoyo-Prats, D. Aubert, A. Sanchez-Garcia, J. Sola, N.  
19 Delsaut, S. Kunesch and C. Menniti (CEFREM laboratory) for helping us during sampling. We  
20 thank Research and Testing Laboratories for kindly providing NGS primer assay list. We  
21 would like to acknowledge the Genotoul bioinformatics platform Toulouse Midi-Pyrénées and  
22 Sigenae group (<http://bioinfo.genotoul.fr>; Toulouse, France) for computing and storage  
23 resources. We also thank D. Ning and N. Xiao for MENAP support  
24 (<http://ieg4.rccc.ou.edu/mena/main.cgi>).

25 **Abstract**

26 Even if Archaea deliver important ecosystem services and are major players in global  
27 biogeochemical cycles, they remain poorly understood in freshwater ecosystems. To our  
28 knowledge, no studies specifically address the direct impact of xenobiotics on the riverine  
29 archaeome. Using environmental DNA metabarcoding of the 16S ribosomal gene, we  
30 previously demonstrated bacteriome significant responses to pollutant mixtures during an  
31 extreme flood in a typical Mediterranean coastal watercourse. Here, using the same  
32 methodology, we sought to determine whether archaeal community shifts were also driven by  
33 environmental stressors during the same flood. Further, we wanted to determine how archaea  
34 taxa compared at different seasons. In contrast to the bacteriome, the archaeome showed a  
35 specific community in summer compared to winter and autumn. We also identified a significant  
36 relationship between *in situ* archaeome shifts and changes in physicochemical parameters  
37 along the flood, but a less marked response to river hydrodynamics than bacteria. New urban-  
38 specific archaeal taxa, which were significantly related to multiple stressors, were identified.  
39 Through statistical modeling of both domains, our results demonstrate that Archaea, seldom  
40 considered as bioindicators of water quality, could provide a rapid assessment of microbial  
41 pollution risk and thus have the potential to improve monitoring methods of watersheds.

42

43 **Keywords:** microbial ecotoxicology; water quality; extreme storm event; coastal  
44 Mediterranean rivers; sewer overflow; environmental DNA; metabarcoding.

## 45        **1. Introduction**

46    In the 1970s, Woese and collaborators highlighted a new domain of life, the Archaea, distinct  
47    from Bacteria and Eukaryota domains (Woese and Fox 1977; Woese et al. 1978). With the  
48    advent of Next Generation Sequencing (NGS), archaeal research and knowledge are expanding  
49    (Adam et al. 2017; Bang and Schmitz 2018). Archaea are recognized as major players in the  
50    global biogeochemical cycles of carbon, nitrogen, hydrogen and sulfur (Casamayor and  
51    Borrego 2009; Offre et al. 2013; Castelle et al. 2015) and there are at least two metabolisms,  
52    essential for nutrient cycling, which are carried out exclusively by archaea: methanogenesis  
53    and anaerobic methane oxidation (Joye 2012). Despite their importance for ecosystem  
54    functioning and their ubiquitous presence (Chaban et al. 2006; Casamayor and Borrego 2009;  
55    Herfort et al. 2009; Auguet et al. 2010), the environmental archaeome has been overlooked for  
56    decades. Most studies have concentrated on marine archaea (Zinger et al. 2012; Zeglin 2015),  
57    and the diversity and importance of archaea in other environments have been largely  
58    disregarded (Casamayor and Borrego 2009; Zinger et al. 2012; Zeglin 2015; Adam et al. 2017).  
59    Only recently, continental freshwater habitats have emerged as one of the largest reservoirs of  
60    archaeal diversity (Auguet et al. 2010; Zinger et al. 2012). Some studies have linked archaeal  
61    communities to water physicochemical properties such as pH, temperature and nutrients  
62    (Herfort et al. 2009; Wang et al. 2018; Lei et al. 2020). *Methanobrevibacter smithii*, for  
63    example, was proposed as a potential indicator of human-specific sewage pollution (Johnston  
64    et al. 2010; McLellan and Eren 2014). To assess water quality, several studies have focused on  
65    freshwater archaea (Cannon et al. 2017; Dila et al. 2018), notably for their potential remediation  
66    role in heavily contaminated urban rivers (Samson et al. 2019; Lei et al. 2020). Cannon *et al.*  
67    (2017) found that a rain event induced changes in the structure of microbial communities,  
68    including archaea, from environmental DNA (eDNA) and stressed the importance of  
69    considering hydrological conditions when studying riverine microbiomes. Both chemical and  
70    microbial pollutants reach surface waters via point sources (such as urban sewage) or diffuse  
71    sources (linked to runoff) of pollution. It is well known that during rainfall events, particles  
72    from terrestrial soils and river basin sediments remobilize, and affect water quality (Garcia-  
73    Esteves et al. 2007; Dumas et al. 2015; Faure et al. 2015) because soils and sediments store  
74    pathogens, nutrients and pollutants. Thus, suspended particles have a crucial role in the transfer  
75    of contaminants to surface waters through runoff and in the resuspension of river sediments  
76    during storms (Turner and Millward 2002; Amalfitano et al. 2017). Moreover, some studies  
77    have reported that riverine archaea tend to be associated with particles and derive only from

78 allochthonous inputs (Crump and Baross 2000; Casamayor and Borrego 2009; Hu et al. 2018).  
79 This is all the more important in Mediterranean regions, where extreme hydrological events  
80 are expected to become more intense and frequent due to climate change (Cowling et al. 2005;  
81 Blanchet et al. 2016). Furthermore, first-flush events during rainfalls lead to Combined Sewer  
82 Overflows (CSOs), which carry large loads of contaminant mixtures over surface waters  
83 through in-sewer solids resuspension (Ashley et al. 1992; Osorio et al. 2012; Oursel et al. 2014;  
84 Reoyo-Prats et al. 2017, 2018). We previously demonstrated that an extreme Mediterranean  
85 flood produced shifts in the particle-attached bacterial compartment from eDNA, severely  
86 affecting resident riverine communities (Noyer et al. 2020). In this study, we went a step further  
87 by using metabarcoding of the 16S ribosomal RNA gene (rDNA) to explore how the diversity  
88 of the particle-attached archaeome changed within the same environmental samples, and to  
89 compare the responses between the bacteriome and the archaeome. Next, we modeled shifts in  
90 both communities using physical parameters as well as several families of chemical parameters  
91 as environmental forces, which is a first in environmental microbiology. This study addressed  
92 the following questions: how did the fluvial particle-attached archaeal community change  
93 between seasons and how did it evolve over the course of a heavy rain event? How our findings  
94 compare to other studies of archaeal alpha and beta diversity in lotic ecosystems? Did  
95 environmental parameters drive structural shifts in the archaeome as they did in the  
96 bacteriome? Was there a strong relationship between key taxa and environmental dynamics?  
97 How did the seasonal and temporal succession of bacterial and archaeal communities compare?  
98 The answer to these questions could, in general, provide insights on the use of microorganisms  
99 in water quality assessment and, in particular, help on the rapid risk assessment of multiple  
100 pollutants in aquatic ecosystems.

## 101 **2. Materials and Methods**

### 102 **2.1. Study site, sampling information**

103 Sampling took place in the Têt River, a watercourse representative of Mediterranean coastal  
104 watercourses with a torrential regime that discharges into the Gulf of Lion (Southeast of  
105 France) (Dumas et al. 2015; Reoyo-Prats et al. 2017) downstream from the Perpignan city  
106 wastewater treatment plant, the main threat to the water quality of this river (Fig. 1a, Conseil  
107 Général des Pyrénées Orientales 2009, 2012; Reoyo-Prats et al. 2017). The Vinça dam, situated  
108 40 km upstream from the sampling station, controls the downstream river flow, particularly

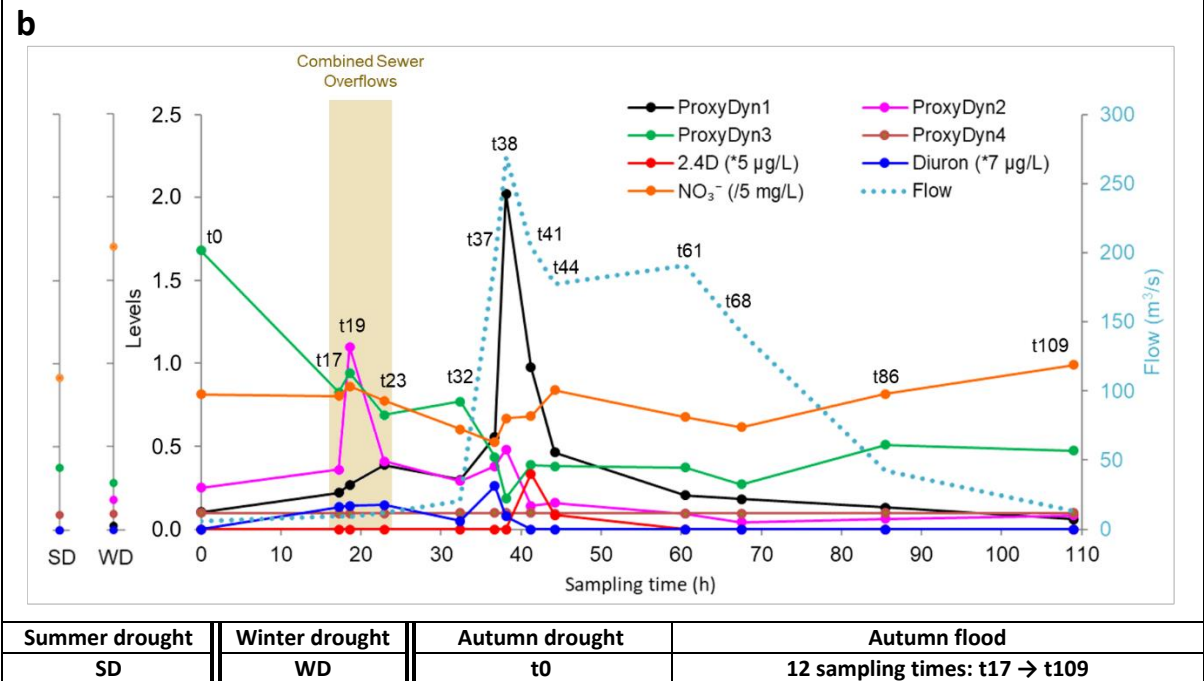
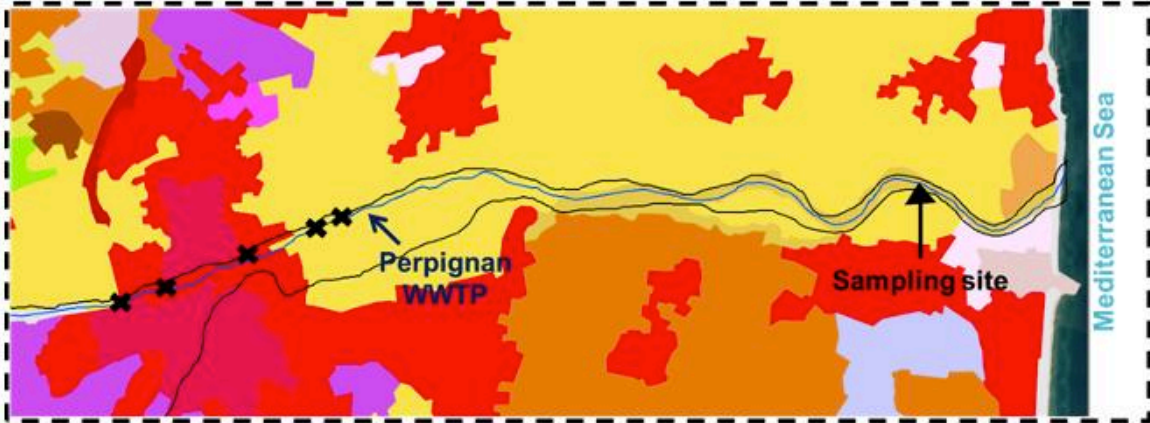
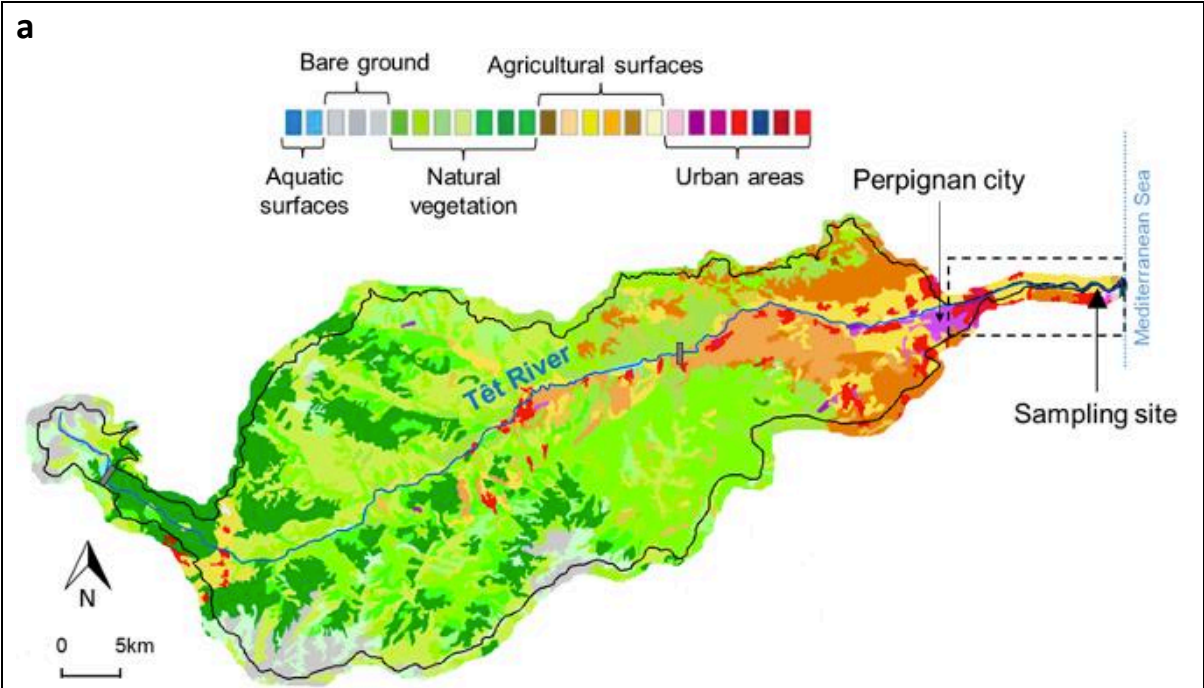
109 during floods. For sampling methodology and sampling site see Reoyo-Prats *et al.* (2017). In  
110 short, ten liters of river water were collected in summer, winter, and autumn, before, during  
111 and after a 5-year flood that we followed 24h/24h during more than 4 days (see Fig. 1b for  
112 further details).

113 First flushes during the flood brought the highest levels of *E. coli* and *Enterococci* ever detected  
114 in this river (Reoyo-Prats *et al.* 2017) as well as relative higher abundance of other typical  
115 sewer bacteria (Noyer *et al.* 2020) and higher levels of dissolved pharmaceuticals (Reoyo-Prats  
116 *et al.* 2018), which indicated the moment at which sewer overflows occurred (Fig. 1b).  
117 Environmental DNA sampling was previously described by Noyer *et al.* (2020). In short, a liter  
118 of mixed-water sample was entirely (or until clogged) filtered through cellulose acetate MF-  
119 Millipore membrane filters with 3  $\mu\text{m}$  porosity (Merck Darmstadt, Germany) and repeated  
120 three times to obtain three replicates per sample.

## 121 **2.2. Nucleic acid extraction, 16S rRNA gene sequencing, and sequence analyses to** 122 **obtain Operational Taxonomic Units (OTUs) contingency table**

123 Nucleic acid extraction and bacterial sequencing from eDNA were described in a  
124 previous study (Noyer *et al.* 2020) and were performed in triplicate per sample. For archaea  
125 sequencing, a single set of DNA replicates from each sample was sent to the Research and  
126 Testing Laboratory (RTL, Texas, USA). Two more replicates were later sent to the Genome  
127 Quebec laboratory (GQ, Montreal, Canada), except for samples t61 and t68 which were only  
128 sequenced once again for technical reasons. DNA from samples t19 and t23 from the first  
129 replicate, which was already sequenced at RTL, was also sent to GQ to be sequenced again for  
130 comparative purposes. Sequencing targeted V3 and V4 hypervariable regions of the 16S rDNA  
131 by using 519wF (5'-CAGCMGCCGCGGTAA-3') and 1017R (5'-  
132 GGCCATGCACCWCCTCTC-3') universal archaeal primers (Borrego *et al.* 2020) and was  
133 performed on an Illumina MiSeq sequencer using a 2x300bp paired-end protocol. Libraries  
134 were generated by pooling equimolar ratios of amplicons before sequencing. In contrast to RTL  
135 sequences, those provided by GQ contained primers. In order to pool sequences together, we  
136 eliminated primers from GQ sequences using Cutadapt version 1.8.3 for Unix (Martin, 2011).  
137 Default options were used with the exception of sequences treatment as paired with -g and -G  
138 options for forward and reverse primers respectively, taking wildcards into account, discarding  
139 untrimmed sequences and setting an overlap of 14 bp, a quality-base of 33 and an error-rate of  
140 0.1. Harmonized sequences were pooled together and archived before being uploaded to the

141 Galaxy platform (Afgan et al., 2016): <http://sigenae-workbench.toulouse.inra.fr>. FROGS  
142 pipeline (v. r3.0-3.0, Escudié et al. 2018) was used to process sequences to form OTUs and to  
143 taxonomically affiliate them as described in Noyer *et al.* (2020) except that VSEARCH (v2.6.2,  
144 Rognes et al. 2016) was used as a read pair assembler, which allows a higher number of  
145 sequences to be conserved when amplicon sizes are highly variable, as was the case for our  
146 dataset. Read length was set to 300pb and the amplicon size was set to 450pb for the minimum  
147 and optimized to 545pb for the maximum. We assigned each OTU up to the species taxonomic  
148 level based on blast alignment using the affiliation tool (v. r3.0-2.0) and the Silva 138.1  
149 database with a pintail score of 100, which allowed for the most accurate affiliation possible.  
150 No archaea hits were removed hereafter. To resolve the taxonomic ambiguity of OTUs that  
151 were multi-affiliated within the FROGS pipeline when using blast against the curated pintail  
152 100 score silva database, we blasted these OTUs against the NCBI 16S nucleotide collection  
153 database using the megablast algorithm.



154 **Fig. 1** Têt River archaeome sampling sites and environmental parameters measured in the same samples. (a)  
155 Watershed of the river with sampling site (black arrow), located after wastewater treatment plan (WWTP) of the  
156 city of Perpignan, combined sewers (black crosses) and water reservoirs indicated as grey rectangles (adapted  
157 from Reoyo-Prats et al. 2017). (b) Environmental parameter dynamics in the Têt River at different seasons and  
158 along an autumn flood. For sample names, see table below figure. Autumn sample names are followed by a  
159 number that indicates the sampling time in hours after t0, which was sampled at autumn basal level water  
160 discharges. Sampling took part at crucial moments of the flood that occurred thereafter: at first flushes (t17-t19-  
161 t23), before the flow peak (t32-t37), during the flow peak (t38-t41), following the release of water from the  
162 upstream Vinça reservoir (t44-t61) and during the return to basal level (t68-t86-t109). ProxyDyn1 corresponds to  
163 the dynamics of particulate organic carbon (/20 mg/l), which represented the dynamics of water flow, also  
164 represented in figure, total suspended solids, total organic carbon, total nitrogen, and terbuthylazine parameters.  
165 ProxyDyn2 corresponds to aminomethyl phosphonic acid (AMPA, µg/l), which represented glyphosate,  
166 phosphate, copper, temperature, *E. coli*, enterococci, diclofenac, sulfamethoxazole and carbamazepine  
167 parameters. ProxyDyn3 corresponds to lead (/150 µg/g) in the representation of the dynamics of cadmium, zinc,  
168 and conductivity parameters. ProxyDyn4 corresponds to pH (/70), which represented cobalt, nickel, and chrome  
169 parameters. Three parameters, Diuron, 2.4D and NO<sup>3-</sup>, had a unique dynamic. For further details on statistical  
170 analyses for environmental parameters, see Noyer *et al.* (2020).

### 171 2.3. Archaeal diversity analyses

172 Diversity analyses were performed using the output OTUs contingency table, tree and  
173 dissimilarity matrices calculated using FROGS as input for *Phyloseq* within R package 1.24.2  
174 (McMurdie and Holmes 2013) and a collection of additional R functions  
175 (<https://github.com/mahendra-mariadassou/phyloseq-extended>). Trimming rare OTUs affects  
176 alpha-diversity measurements sensitive to rare OTUs such as Chao1, Observed richness and  
177 Shannon indices, while rarefaction is controverted as well when concerning some alpha  
178 diversity indices (McMurdie and Holmes 2014; Cameron et al. 2021). Alpha diversity was  
179 therefore calculated using non-filtered and non-normalized replicates from the GQ laboratory  
180 only, because the lower sequence depth of RTL sequenced replicates precluded comparison.  
181 Fisher, Simpson, Shannon, and Pielou alpha diversity indices were used, together with the  
182 nonparametric Chao1 species richness estimator. These indices provide complementary  
183 information regarding evenness and richness aspects of alpha diversity that are interesting to  
184 take into account (see, for instance, Walters and Martiny 2020). Kruskal-Wallis test (KW)  
185 followed by a post hoc Dunn test with R software (v. 3.5.1, R Core Team 2018) were applied  
186 to evaluate diversity changes through time. Beta diversity was assessed on all replicates,  
187 independently of platform origin, because sequencing depth is not relevant in this case.  
188 Singletons were filtered out and then abundance was normalized to the sample with the lowest  
189 number of sequence reads. Using this dataset, relative abundances by phylum and class were  
190 plotted. To detect potential outliers in the dataset we proceeded by (i) checking the number of  
191 sequences of each replicate, (ii) checking OTU abundance distribution among replicates of the  
192 same sample and (iii) calculating qualitative Jaccard and quantitative Bray-Curtis  
193 dissimilarities from replicates separately and using Principal Coordinates Analysis (PCoA) to

194 visualize replicate dissimilarities. Once outliers checked, beta dissimilarities were recalculated  
195 on the averaged OTU abundances. To this end, the number of OTUs decreased to less than  
196 10,000 after the dataset was normalized, thus allowing qualitative Unifrac and quantitative  
197 Weighted-Unifrac (W-U) dissimilarities, which also consider phylogeny of OTUs, to be  
198 included within FROGS. PCoA and hierarchical clustering Ward.D2 methods were used to  
199 visualize archaeal community dissimilarities among samples. A one-way analysis of similarity  
200 (ANOSIM, Clarke 1993) was performed to test significant differences between sample groups  
201 resulting from hierarchical clustering. To further check for significant differences in archaeal  
202 community shifts at the class level, the Mann-Whitney test (MW) was implemented with R  
203 software.

## 204 **2.4. Statistical analyses for inference**

### 205 2.4.1. Constrained (canonical) ordination analyses by environmental parameters dynamics

206 Physicochemical environmental parameters were previously measured (Reoyo-Prats et al.  
207 2017) in the same samples in which nucleic acid extractions were performed. Measured  
208 parameters included pH, temperature, conductivity, flow, total suspended solids, particulate  
209 organic carbon, total organic carbon, nitrogen and 250 pesticide molecules, 90  
210 pharmaceutically active compounds, polycyclic aromatic hydrocarbons and polychlorinated  
211 biphenyls, nutrients, trace metals in the particulate fraction and fecal indicators (load in  
212 *Escherichia coli* and Enterococci). Collinearity issues resolution and the seven major  
213 environmental dynamics retained for further analyses are described in Noyer *et al.* (2020). For  
214 clarity, the retained variables that will be used for further analyses as proxies of correlated  
215 environmental variables are summarized in Fig. 1b. Constraint-based ordination analyses were  
216 then used to evaluate the relationships between the normalized OTU contingency table and  
217 retained environmental parameter dynamics using *vegan* R package version 2.5-3 (Oksanen et  
218 al. 2018). Detrended correspondence analysis (DCA) performed on the OTU dataset rendered  
219 a first axis gradient length of 3.7, so both canonical correspondence (CCA) and redundancy  
220 analyses (RDA) were performed (ter Braak 1988). We also performed a Hellinger transformed-  
221 based RDA (tbrDA) (Legendre and Gallagher 2001) and a distance-based RDA (dbRDA)  
222 using all beta dissimilarities from the previous section. Permutation analyses of variance were  
223 used to evaluate the significance of constraint-based models, axes, and variables. Variables  
224 were tested by adding each of them independently and the number of permutations was set to  
225 10,000. To further determine which OTUs best responded to environmental variables, we  
226 reduced the OTU matrix to a percentage of abundance so that CCA/RDA modeling became

227 significant. Instead of 0.005%, as reported by Bokulich *et al.* (2012) and Noyer *et al.* (2020)  
228 for bacteria, we found a percentage of 0.05% for the archaeal dataset. RDA modeling of OTUs  
229 with  $\geq 0.05\%$  of the total read number (i.e. keeping 2,688,328 reads), allowed for the OTU  
230 goodness of fit (GOF) to be calculated. As for bacteria, OTUs retained for further analyses had  
231 a  $GOF \geq GOF_{\text{average}}$ , which is considered a conservative approach to OTU selection.

#### 232 2.4.2. Network construction via module eigengene analysis

233 We used the Molecular Ecological Network Analyses Pipeline (MENAP:  
234 <http://ieg4.rccc.ou.edu/MENA/>) to build the relationships among OTUs following the  
235 developer's recommendations (Deng *et al.* 2012; Tao *et al.* 2018) but sample-specific OTUs  
236 were kept for network construction by changing "OTUs present at least in one sample". An  
237 automatically generated similarity threshold value (0.32) was obtained with Random Matrix  
238 Theory (RMT)-based method, which allowed network construction ensuring that the  
239 connections between microorganisms were non-random ( $R^2$  of power-law = 0.28). The network  
240 was separated into modules via the short random walk method (Pons and Latapy 2005), which  
241 had the highest modularity (0.078) (Newman 2004). Module higher-order organization was  
242 then performed via eigengene analysis (Langfelder and Horvath 2007) using default parameters  
243 to obtain the correlation significance between modules and environmental parameters  
244 dynamics. Cytoscape software (v. 3.7.1, Shannon *et al.* 2003) was used to visualize this  
245 constraint-based network. We also used MENAP to explore the relationship between OTUs  
246 from Bacteria (from the previous study by Noyer *et al.*, 2020) and Archaea domains and flood  
247 environmental dynamics. The network was constructed with the same parameters as before  
248 except zero counts were replaced "by 0.01" instead of "on paired values", to avoid losing an  
249 important number of OTUs when using the matrix of joined OTUs from both domains. The  
250 highest modularity was obtained via the leading eigenvector method (0.520). The RMT  
251 threshold was 0.940 and the  $R^2$  of power law = 0.863.

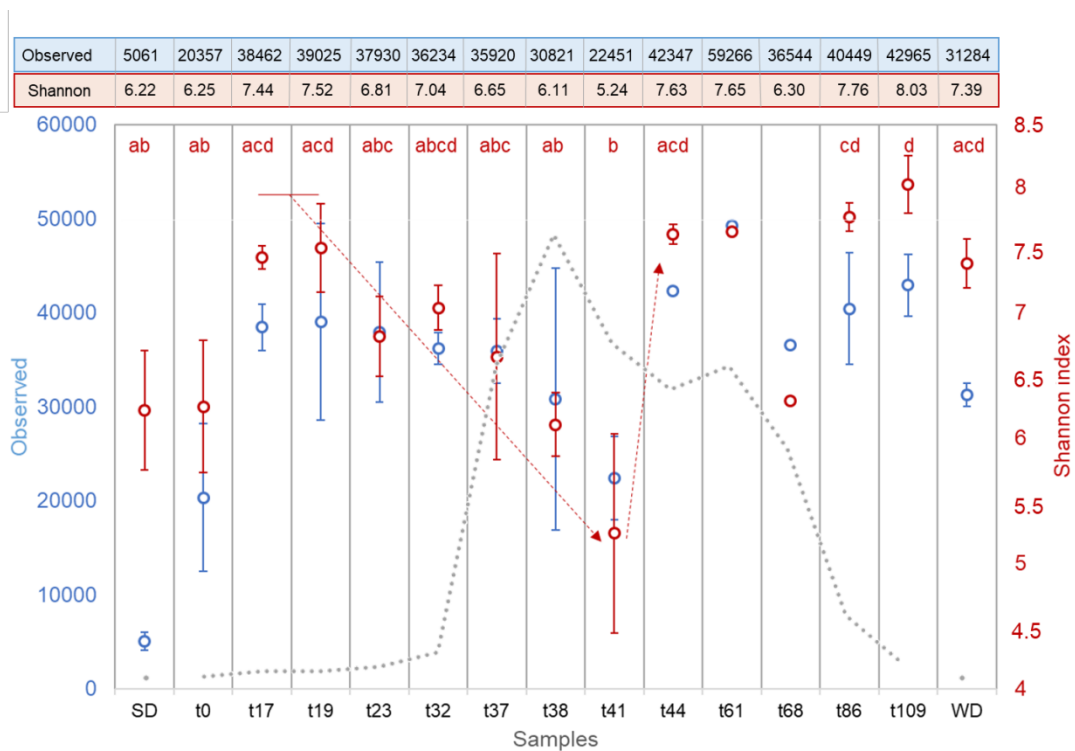
### 252 3. Results

#### 253 3.1. Changes in particle-attached archaeal diversity along a storm event in the Têt 254 River

255 To study changes in an urban archaeome along a storm event, a high-resolution environmental  
256 DNA sampling from river water was performed during a major flood that occurred in autumn  
257 2013. Two other seasons were also sampled during the summer and winter drought periods.

258 All reported sequence data passed standard quality controls of certified sequencing companies.  
 259 A total of 1,804,302 reads corresponding to 350,106 operational taxonomic units (OTUs) were  
 260 identified. Most OTUs (98%) were assigned to the archaeal domain, the rest were eliminated  
 261 from further analysis.

262 Alpha diversity statistical analyses showed significant differences among samples for Shannon  
 263 (KW = 0.03, Fig. 2) and Pielou (KW = 0.03, Table S1) indices only. These two indices changed  
 264 similarly along seasons and during the flood, with equivalent significant differences between  
 265 samples except for the Pielou index for the summer drought, which was significantly higher  
 266 than the flow peak (t38-t41) indicating a greater evenness in OTU abundances in this sample.  
 267 In general, both indices decreased significantly at t41, i.e. right after the flood peak, with  
 268 respect to t17 and t19. Three hours later, a significant increase in diversity was noticed (t44).  
 269 Even if the observed OTU number, Chao1 and Fisher indices did not show significant  
 270 differences (Table S1), they had the same change pattern as the Shannon index (Fig. 2), except  
 271 for a much lower value in the summer drought sample. This result contrast with the Pielou and  
 272 Simpson indices (Table S1), which emphasize the evenness component of diversity, as opposed  
 273 to Fisher and Shannon indices, which appear more related here to the richness component of  
 274 diversity (Magurran 2004).

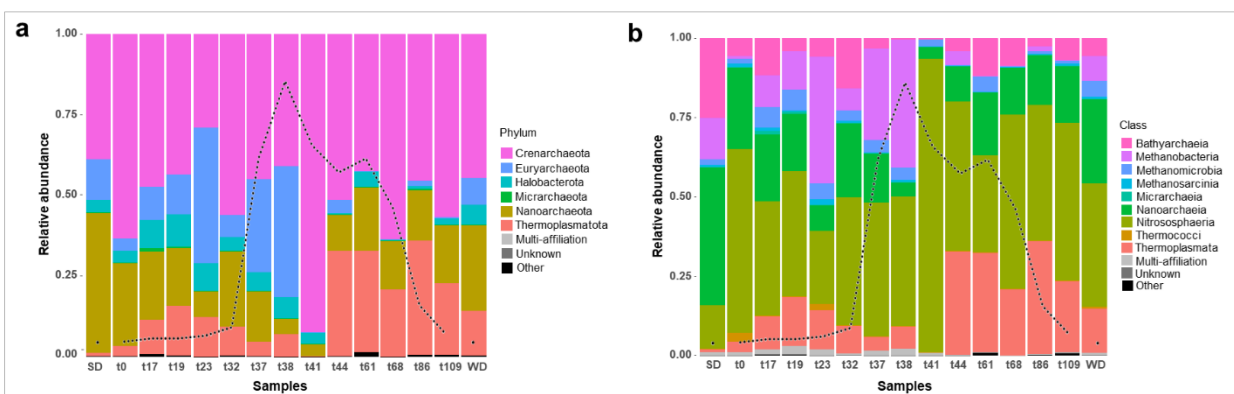


275  
 276 **Fig. 2** Alpha diversity of the archaeome of the Têt river along time. Changes in observed OTU number (blue) and  
 277 Shannon index (red) along the flood (tX) and at summer and winter droughts (SD and WD respectively). For the

278 Shannon index, different letters indicate a significant difference between samples (dunn.test<0.025) and red  
 279 arrows show major significant differences. Observed OTU number was not significantly different (KW=0.14).  
 280 The dotted profile is the flow level at each sampling point (see Fig. 1, also for sample names). Even though the  
 281 absence of replicates for t61 and t68 samples impeded statistical testing, they are represented through time for  
 282 comparison.

283

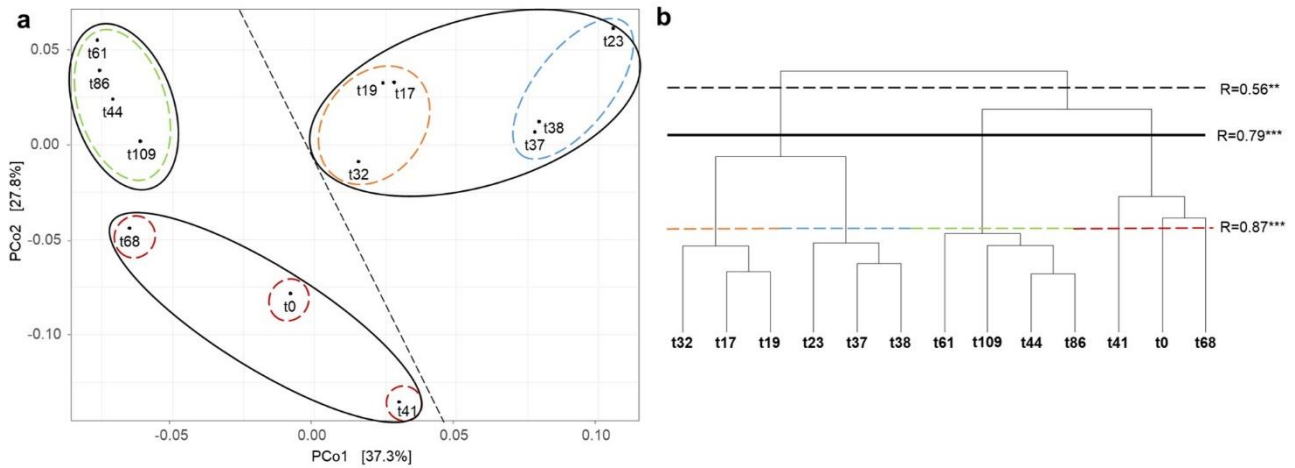
284 After normalization of OTU matrix once singletons were excluded, a total of 1,377 OTUs  
 285 (3,777 sequences/sample) were retained for further analyses. We noticed a great difference in  
 286 the taxonomic composition of the summer drought (SD) with respect to all other samples. SD  
 287 had a significantly lower amount of Nitrososphaeria and Thermoplasmata classes when  
 288 compared to all samples (Fig. 3, MW p=0.012 and p=0.021 respectively) and a higher amount  
 289 of Nanoarchaeia (Nanoarchaeota phylum, Fig. 3) and Bathyarchaeia (Crenarchaeota phylum)  
 290 classes when compared to most samples. These large differences in the summer sample  
 291 community were confirmed with the beta diversity analyses (data not shown), as all samples  
 292 significantly separated from the SD sample with all beta dissimilarity indices, contrarily to  
 293 WD, which always clustered with t17, t19, and t32. Additionally, the taxonomic composition  
 294 of the WD sample was very similar to t17, t19, and t32 samples, mainly composed of  
 295 Nitrososphaeria class, followed by Nanoarchaeia, Thermoplasmata, and then three classes,  
 296 Methanobacteria (Euryarchaeota phylum), Methanomicrobia (Halobacterota phylum) and  
 297 Bathyarchaeia at variable smaller abundances (Fig. 3).



298 **Fig. 3** Composition of archaeal communities averaged across replicates. Histogram of relative abundances (a) of  
 299 the six major phyla and (b) of the ten major classes. Samples are organized according to sampling time from left  
 300 to right: summer drought (SD), autumn flood (sample names are followed by a number that indicates the sampling  
 301 time in hours after the beginning of the flood at t0), and winter drought (WD). The dotted profile is the flow level  
 302 at each sampling point (see Fig. 1 for further details).

303

304 Given these results, only flood samples were used to further explore structural diversity  
305 changes using beta dissimilarities. These samples comprised a total of 1,739 OTUs (19,355  
306 sequences/sample) after eliminating singletons and normalization. Using different beta  
307 dissimilarities allowed for a better assessment of which differences are responsible for the  
308 community structure (either presence/absence or abundance and/or phylogeny of OTUs).  
309 Using only OTU presence/absence with Jaccard qualitative dissimilarity, three communities  
310 were significantly differentiated (Fig. S2.1a). The first community group included samples  
311 collected at t0, t17, t19 and t32, the second included samples t23, t37, and t38, and the third  
312 included the rest of the samples (t41-t109), which was the most differentiated cluster. But when  
313 phylogenetic relationships were considered using Unifrac qualitative dissimilarity, t41 sample  
314 grouped with t23, t37 and t38 instead (Fig. S2.1b). With Unifrac, this last cluster was the most  
315 differentiated. When Bray-Curtis quantitative dissimilarity, which considers OTU abundance,  
316 was used, three community groups of samples were distinguished (Fig. S2.1c). The first  
317 included from t17 to t38 samples, the second included t0, t41, and t68 samples, and the third  
318 t44, t61, t86, and t109 samples. When considering phylogenetic relationships using W-U,  
319 observed community groups coincided with those of Bray-Curtis dissimilarity (Fig. 4, bold  
320 black line), but the most significantly differentiated communities were those from the group of  
321 t23, t37 and t38 (axis 1) and then t41 and t0 samples (axis 2). Even though the first taxonomic  
322 changes occurred from the first flood sample at t17, samples t23, t37 and t38 had a particular  
323 significant increase in Methanobacteria (Euryarchaeota phylum) (Fig. 3, MW,  $p=0.001$ ).  
324 Sample t0 differentiated significantly from samples from the end of the flood (from t44 to  
325 t109) only when considering OTUs presence/absence but not when abundance alone or with  
326 phylogeny were considered. This sample had a significantly lower abundance of taxa from the  
327 Thermoplasmata class with respect to that group of samples (Fig. 3b, MW  $p=0.003$ ). Regarding  
328 t41 sample community, it had a particular taxonomy, significantly dominated by  
329 Nitrososphaeria class (MW  $p=0.002$ ) and W-U dissimilarity significantly separated t41 from  
330 the rest of the samples (Fig. 4). With regard to the group of samples at the end of the flood  
331 event, from t44 to t109, we could notice a significant increase of Thermoplasmata class with  
332 respect to all other flood samples (Thermoplasmata phylum, MW  $p=0.002$ , Fig. 3b).  
333



334 **Fig. 4** Structure of archaeal communities averaged across replicates. (a) Principal Coordinate Analysis (PCoA)  
 335 and (b) hierarchical clustering with Ward D2 linkage method using Weighted-Unifrac dissimilarity computed on  
 336 OTU average abundance. Lines indicate ANOSIM significant groups. Sample names are followed by a number  
 337 that indicates the sampling time in hours after t0 (see Fig. 1 for details). Significant codes \*\* and \*\*\* indicate p-  
 338 value < 0.01 and < 0.001, respectively.

339

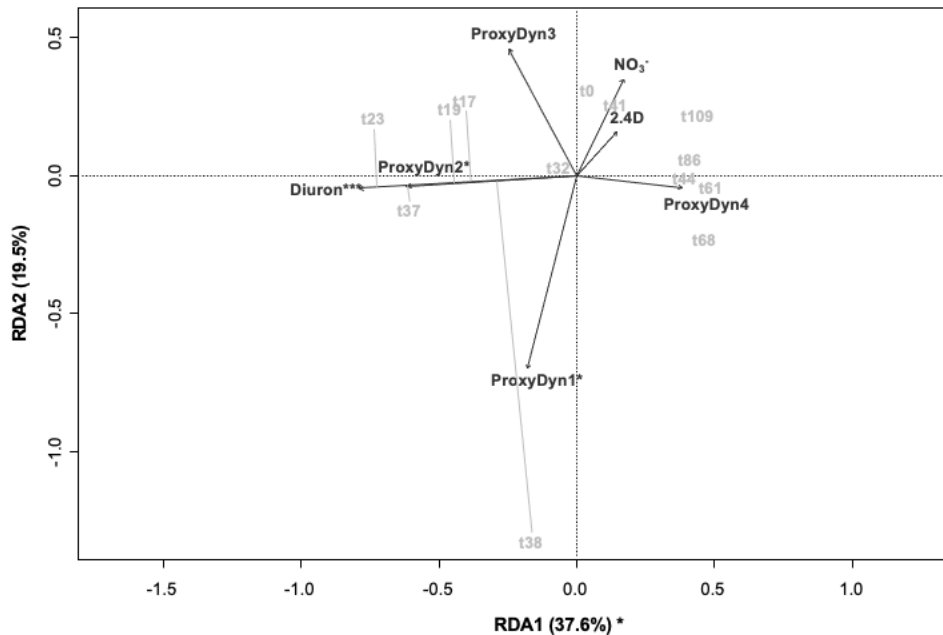
340 **Table 1** Summary of constraint-based multivariate statistical models on archaea OTU matrix averaged over  
 341 replicates and without singletons. (a) Permanova significance of the five models tested and the percentage of  
 342 biological variance that is explained by each model using permutation test with anova.cca function. (b) Axes and  
 343 modeled variables significance after permanova using anova.cca of significant models in (a). Axes not shown  
 344 were not significant. p-values significance codes: (\*\*\*) < 0.001 < \*\* < 0.01 < \* < 0.05).

a	OTUs matrix transformation	Model significance	Variance (%)	b								
				Axes significance and variance explained (%)		Statistical significance of modeled variables						
				CAPI	ProxyDyn1	ProxyDyn2	ProxyDyn3	ProxyDyn4	2.4D	Diuron	NO <sub>3</sub> <sup>-</sup>	
dbRDA	Jaccard	0.003**	63.38%	0.002** (22.74)	0.001***	0.002**	0.001***	0.105	0.095	0.001***	0.096	
	Unifrac	0.008**	66.35%	0.040* (30.24)	0.001***	0.021*	0.046*	0.458	0.383	0.036*	0.014*	
	Bray-Curtis	0.326	60.04%	0.006** (42.89)	0.006**	0.009**	0.039*	0.050*	0.004**	0.002**	0.166	
	Weighted-Unifrac	0.004**	76.58%									
CCA		0.765	56.44%									
RDA	Hellinger	0.134	61.4%									

345

### 346            **3.2. Modeling archaeome diversity according to multiple contaminant dynamics**

347    Constrained multivariate analyses were performed to determine if the retained environmental  
348    dynamics (Fig. 1b) could statistically explain the observed community structure and diversity  
349    shifts through time. Significance and percentage of variance explained by all models tested  
350    were summarized in Table 1a. Jaccard, Unifrac and Weighted-Unifrac dbRDAs supported  
351    significantly (p-value < 0.01) a link between environmental parameters included in the model  
352    and our community data (Fig. S2.2). Models using Jaccard and Unifrac dissimilarities  
353    explained between 63 and 66% of the total variance, respectively. Only the first canonical axis  
354    was significant in both models, with a higher proportion of the variance in the dissimilarity  
355    matrix explained when phylogeny was considered using Unifrac (33% vs 23% for Jaccard, Fig.  
356    S2.2a-b). In both models, the same four environmental dynamics were significant, ProxyDyn1,  
357    ProxyDyn2, ProxyDyn3, and Diuron (Table 1b). W-U dbRDA model performed best,  
358    explaining 78% of variance in the OTU matrix. The first axis was significant and explained  
359    44% of the total variance. Four environmental dynamics were significant according to this  
360    model, ProxyDyn1, ProxyDyn2, 2,4-Dichlorophenoxyacetic acid (2,4D), and Diuron (Table  
361    1b, Fig. S2.2c). Finally, only when the raw matrix was reduced to OTUs  $\geq 0.05\%$  of total read  
362    number (see section 2.4.1 for details) tBRDA became significant (p-value = 0.046, DCA first  
363    axis length < 3), with one significant axis and three significant dynamics, ProxyDyn1 (p-value  
364    = 0.032), ProxyDyn2 (p-value = 0.007) and Diuron (p-value = 0.001) (Fig. 5). This matrix  
365    included 53 OTUs, and 284,506 reads, i.e. 3% of total OTUs, representing 69% of the total  
366    reads) which were conserved for further analyses. This model explained 66.32% of the total  
367    variance, and the first axis was significant and explained 37.6% of the variance. Samples well  
368    projected to ProxyDyn2 and Diuron were t23 and t37, followed by t17 and t19, and to a lesser  
369    extent t38 (see Fig. 5), which was well projected to ProxyDyn1. Notice however that axis 2  
370    was not significant.



371

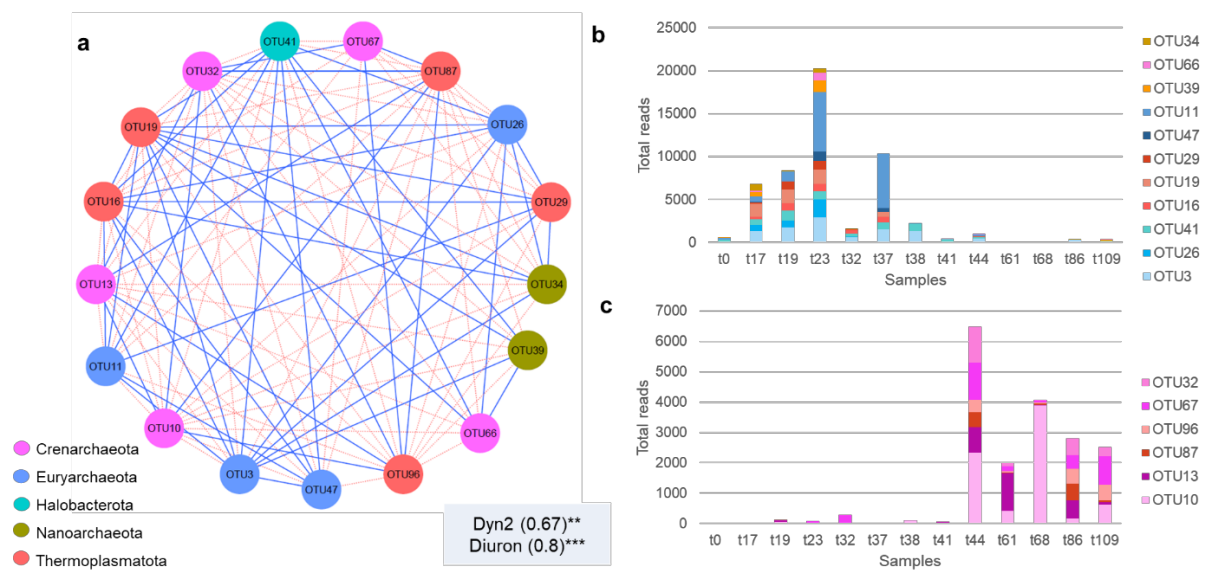
372 **Fig. 5** Redundancy analysis (RDA) biplot with scaling by sites on the normalized matrix of OTUs with an  
 373 abundance  $\geq 0.05\%$ . The model explained 66.32% of the variance ( $p < 0.05$ ). Significance for axes and  
 374 environmental dynamics after permanova analyses are indicated, p-value significance codes:  
 375 \*\*\* $< 0.001$  \*\* $< 0.01$  \* $< 0.05$ . Sample names are followed by a number that indicates the sampling time in hours  
 376 after the beginning of the flood at t0. For further details on sample names and retained environmental variable  
 377 dynamics, see Fig. 1b. Perpendicular grey lines represent the projection of the corresponding samples onto the  
 378 corresponding dynamics and approximate the value of that sample along the variable (Legendre and Legendre  
 379 2012).

### 380 3.3. Constrained molecular ecological network analyses by environmental 381 parameters dynamics

#### 382 3.3.1. Archaeal network

383 Network analysis using MENAP resulted in four modules containing all OTUs and 774 links.  
 384 Module eigengene analysis allowed correlation of modules with environmental variables. Only  
 385 one module was significantly correlated to the environmental dynamics of the flood,  
 386 particularly with ProxyDyn2 and Diuron (Fig. 1b). This module included 28 OTUs of which  
 387 17 had a significant module membership (Fig. 6a), comprised of 11 with positive (52,149  
 388 reads) and six with negative (18,573 reads) correlations (Table S3.1). Worth noting is that  
 389 OTUs with positive module membership (Fig. 6b) had positive interactions with each other  
 390 (Fig. 6a) and negative interactions with OTUs with negative module membership (Fig. 6c), and  
 391 OTUs with negative module membership had positive interactions with each other and negative  
 392 interactions with OTUs with positive module membership. All positively correlated OTUs  
 393 were abundant in samples t23 (20,246 reads, which represent 39% of reads along the flood

394 from these OTUs, Table S3.1), t37 (20%), t19 (16%) and t17 (13%). A total of 60% of reads  
 395 from these OTUs belonged to the Methanobacteria class (Euryarchaeota phylum). Two OTUs  
 396 were particularly abundant, OTU3, matching *Methanobrevibacter (Mbr.) smithii* at 99%  
 397 similarity after blastn search against NCBI database, and OTU11 matching *Methanobacterium*  
 398 (*Mba.) palustre* (100%). The next most abundant OTUs also matched methane-related taxa:  
 399 OTU41, which matched *Methanosaeta (Msa.) concilii*, 100%, from Halobacterota phylum),  
 400 OTU19 (*Methanogranum* sp. 98.04%. from Thermoplamatota phylum), OTU26 (*Mbr.*  
 401 *acidurans*, 99%, from Euryarchaeota phylum) and OTU16 (Methanomethylphilacea, 99.61%,  
 402 from Thermoplamatota). The other positively correlated OTUs (not highlighted in bold in  
 403 Table S3.1) did not match any further than the family level after a blast search of the NCBI  
 404 database. Finally, negatively correlated OTUs were abundant in samples from the end of the  
 405 flood (t44-t109) and belonged to Nitrososphaeria (Crenarchaeota phylum, representing 85% of  
 406 the sequences of these OTUs) and Thermoplasmata (15%) classes (Thermoplasmata  
 407 phylum).



408

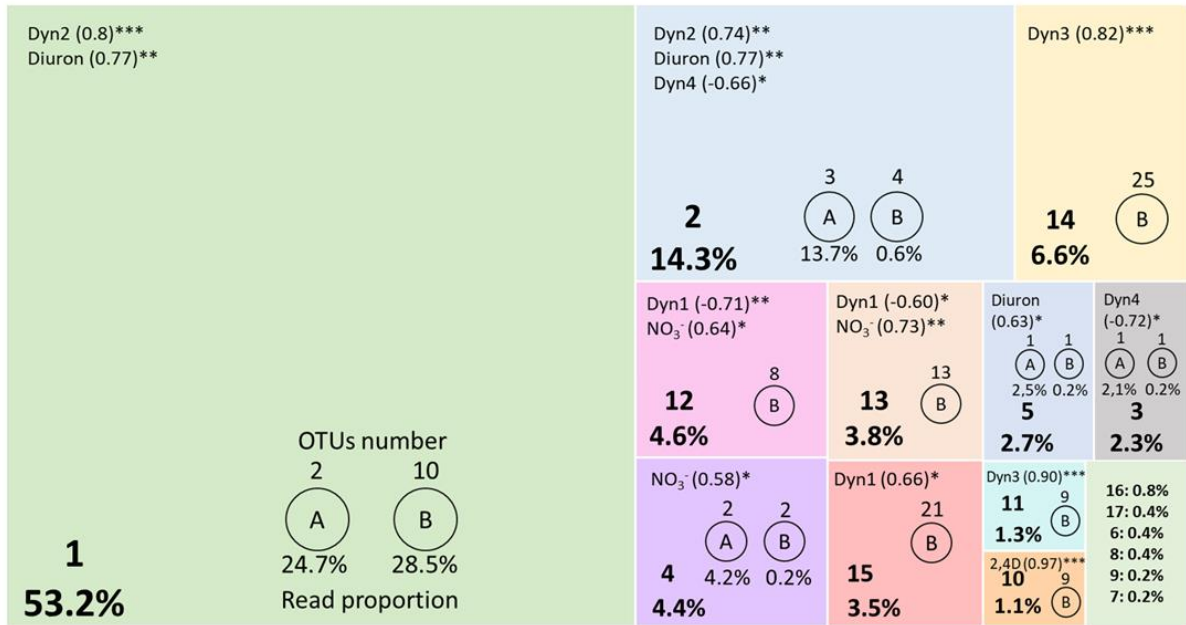
409 **Fig. 6** (a) Molecular ecological network of the unique module significantly positively correlated with  
 410 environmental dynamics, particularly ProxyDyn2 and Diuron (see Fig. 1b for details and sample names). (b)  
 411 Histogram of total reads of OTUs with positive module membership in function of samples along the flood. (c)  
 412 Same for OTUs with negative module membership. Environmental dynamics are followed by module correlation  
 413 value between parenthesis and the p-value significant code as follows: \*\*\*<0.001<\*<0.01<\*<0.05. OTUs are  
 414 colored according to their phylum. The positive and negative connectivities between OTUs are indicated by blue  
 415 and red lines, respectively. Only OTUs with a significantly correlated abundance profile with module are  
 416 represented in this figure.

417

### 418 3.3.2. Archaeal and bacterial joining network

419 To further explore the microbial relationships with environmental parameters, we performed a  
420 second eigengene analyses by first constructing a network using the 53 retained archaeal OTUs  
421 from this study, and the 260 retained bacterial OTUs from the previous study using the same  
422 samples and methodology (Noyer et al. 2020). The network we obtained before considering  
423 environmental parameters consisted in 200 nodes (OTUs) and 967 links and was composed of  
424 21 modules. When considering environmental parameters, the network was composed of 136  
425 OTUs, 442 links and 13 modules (Fig. 7, Table S3.2). All retained environmental dynamics  
426 (Fig. 1b) were positively or negatively correlated with one or more modules and there were  
427 127 bacterial and 9 archaeal significant OTUs. More than half of the total reads (53%) were  
428 represented in module 1 (Fig. 7). Archaeal OTUs were present in five modules (Fig. 7). Six  
429 archaeal OTUs represented 41% of the total reads among significant OTUs in the network and  
430 were linked to ProxyDyn2 and/or Diuron. Notably, OTU3 and OTU41 in module 1, OTU16,  
431 OTU26, and OTU61 (*Mba. acidurans*, 98.42%) in module 2, and OTU47 (*Mba. formicicum*,  
432 100%) in module 5 (Table S3.2). They were mainly present in t17, t19, t23, and t37 samples.  
433 Two archaeal OTUs, 94 and 44, in module 4 correlated to  $\text{NO}_3^-$  (4% of the total reads, Fig. 7),  
434 and belonged to Nitrosotaleaceae family (Crenarchaeota phylum) and were mainly present  
435 towards the end of the flood event. Of the 127 bacterial OTUs present in this joined network,  
436 49 were present in the bacterial only network from the previous study (Noyer et al. 2020, in  
437 purple in Table S3.2) and were significantly linked to the same environmental dynamics. Worth  
438 noting is that the bacteria in modules which were positively correlated with ProxyDyn2 and  
439 Diuron were also the most relatively abundant in t17, t19, t23, and t37 samples. The most  
440 abundant of these bacterial OTUs was OTU5, which matched *Arcobacter cryaerophilus* and  
441 represented 20% of the total reads included in the network.

442



443

444

445

446

447

448

449

450

451

**Fig. 7** Summary of joined bacterial and archaeal network analysis. Each colored rectangle represents a module whose number appears at the bottom left corner of each rectangle together with the percentage of reads in the module out of the total number of reads analyzed within the network. The number of OTUs and the proportion of reads within each module for each domain: archaea (A) and bacteria (B) are also indicated in each rectangle. At the top left of each rectangle the environmental dynamics are indicated with module eigengene correlation value between parentheses and the p-value significant code as follows: \*\*\*<0.001<\*\*<0.01<\*<0.05. The rectangle on the bottom right corner represents the six modules whose percentage of reads is less than 1% of the total number of reads analyzed in the network.

452

## 4. Discussion

453

454

### 4.1. Particle-attached archaeome diversity at three different seasons was higher and more even than in all other lotic ecosystems studied so far

455

456

457

458

459

460

461

462

463

464

Archaea have been studied in only a few river environments (Herfort et al. 2009; Hu et al. 2016, 2018; Cannon et al. 2017; Samson et al. 2019; Lei et al. 2020; Cao et al. 2020; Pinto et al. 2020; Shen et al. 2021) and to the best of our knowledge, no study has characterized their diversity over different seasons in lotic ecosystems. Here, eDNA was extracted from riverine water samples from summer, autumn, and winter and characterized using high-throughput Illumina sequencing of the archaeal rDNA in a coastal Mediterranean watercourse, the Têt River (Southeast France). Shannon alpha diversity (Fig. 2) from summer, winter and autumn drought samples were not significantly different (SD = 6.22; t<sub>0</sub> = 6.25 and WD = 7.39). This was also the case for all alpha diversity indices (Table S1). Lei *et al.* (2020) obtained lower values of Shannon index (ranging 4.07-5.72) through Illumina sequencing of a highly polluted

465 river in China. Along a river in India sampled during summer and sequenced by metagenomic  
466 analyses, Samson *et al.* (2019) found a Shannon diversity varying from 3.12 to 4.79, depending  
467 on the sampling site. Hu *et al.* (2018) studied microbial diversity in a high-elevation river in  
468 China using universal primers and found even lower Shannon values for archaea along the river  
469 (2-2.7) and a Pielou evenness index very high (0.77-0.82) compared to ours (ranging 0.44-0.51  
470 in Têt drought samples along seasons). These authors used 97% identity to define OTUs, while  
471 the other two studies did not specify how they defined the OTUs in their studies. Nevertheless,  
472 given the lower number of OTUs retained in these studies, the differences in alpha diversity  
473 with respect to our study could be due to less throughput sequencing. Borrego *et al.* (2020)  
474 studied particle-attached archaea in a Mediterranean water reservoir in summer with the same  
475 specific primers as in the present study, and they also found a lower Shannon alpha diversity  
476 than ours ( $4.9 \pm 0.15$ ). Gobet *et al.* (2014), in a comparative study of different alpha diversity  
477 indices between ARISA versus pyrosequencing methodologies, determined significant  
478 correlation results among methods, particularly with Shannon index, without a need for  
479 correction for sequencing depth. In summary, although the Têt River archaeal diversity was  
480 higher and less even (lower Pielou index) when compared to other riverine environments  
481 studied so far, additional studies with higher throughput and standardized sequencing pipeline  
482 analyses are needed to better understand the ecology of fluvial archaea.

483 Studies on lotic ecosystems have revealed the presence of three major phyla, Crenarchaeota,  
484 Euryarchaeota and Thaumarchaeota using the previous silva database (Hu *et al.* 2016, 2018;  
485 Samson *et al.* 2019; Lei *et al.* 2020). When considering archaeal taxonomy changes since the  
486 last silva database release, the major phyla observed in the Têt river corresponded to those  
487 same phyla, but we also found the Nanoarchaeota phylum (Fig. 3a). In a recent study, which  
488 used the same primers as those used in our study, Woesarchaeia class (now called  
489 Nanoarchaeia) was found in a small water reservoir sampled in summer (Borrego *et al.* 2020).  
490 In our study, the summer drought community showed, through beta diversity analyses, the  
491 greatest difference with respect to communities present in autumn and winter and was also  
492 dominated by this class of the Nanoarchaeota phylum, followed by Bathyarchaeia class  
493 (Crenarchaeota phylum). Primer bias could thus be responsible for the absence of this class in  
494 previous riverine studies. Nevertheless, winter drought and dry autumn weather (t0) samples  
495 had a smaller proportion of these classes at the expense of Nitrososphaeria class  
496 (Crenarchaeota phylum, Fig. 3). On the other hand, Herfort *et al.* (2009) sequenced five  
497 DGGE fragments amplified from surface waters of the Têt River in June 2005 that matched  
498 two classes, a marine benthic group Crenarchaeota and LDS/RCV from Halobacteriales order

499 (currently at Halobacteria class from Halobacterota phylum). In this study, we also found taxa  
500 from the genus *Methanomicrobia*, which were present in all samples independently of season,  
501 and are classified within Halobacterota and thus closely related to Halobacteria. While we also  
502 found taxa from the marine benthic group A from Crenarchaeota phylum (not shown), they  
503 were absent in the summer drought. Given the technical limitations of the DGGE fingerprinting  
504 method, a biased result cannot be discarded.

#### 505 **4.2. Particle-attached archaeome shifts gave evidence of allochthonous inputs into** 506 **the Têt River along a Mediterranean extreme flood**

507 In this manuscript, we characterized the temporal shift of the particle-attached riverine archaeal  
508 community throughout an autumn storm event that included a 5-year flood and led to an  
509 instantaneous peak discharge of 270 m<sup>3</sup>/s. Cannon *et al.* (2017) is the only study that  
510 characterized river archaeal composition in water samples from a contaminated urban river  
511 before and after transient rainfall using Illumina sequencing of the rDNA. They found a weak  
512 resolution in archaeal sequences of samples from before and after the rain event, which they  
513 concluded might be due to a primer bias. In this study, we demonstrated major changes in  
514 archaeal taxonomy, and therefore community shifts observed through beta diversity, occurred  
515 at specific moments along the flood event and not when comparing samples from before and  
516 after the flow peak. It is therefore possible that the absence of differences in Cannon *et al.*  
517 (2017) was due to the resilience of archaeal communities at the end of the rainfall as was the  
518 case at the Têt River. Communities from the end of the flood, from t44 to t109 were indeed  
519 more similar to the t0 sample (sampled before the rainfall started, see Fig. 4). A first shift in  
520 the structural diversity occurred after t17, particularly in samples t23 and t37. These samples  
521 corresponded to moments of multipollution peaks that occurred at storm first flushes CSOs and  
522 inputs from in-sewer sediment resuspension (Fig. 1b, see also Reoyo-Prats *et al.* 2017).  
523 Methane-related classes such as Methanobacteria, Methanomicrobia and Methanosarcinia  
524 became significantly abundant at these moments, and our results support these classes as major  
525 components of riverine communities related to pollutants, organic matter inputs and/or hypoxic  
526 sediments, as reported by Casamayor and Borrego (2009) with respect to the Euryarchaeota  
527 phylum. All these classes belonged indeed to the Euryarchaeota before the last silva database  
528 release. Lei *et al.* (2020) also found a predominance of different Euryarchaeota methanogens  
529 in water samples from a black odor, highly polluted Chinese river and more particularly the  
530 large presence of *Methanobacterium* genus (Methanobacteria class) in water as well as in hotter

531 and lower-oxygen, downstream sediments, what corroborates our hypothesis on the origin of  
532 this river community shift. A second major community shift during the storm event occurred  
533 at t41, just after the maximum water discharges (Fig. 3). Compared to Lei *et al.* (2020), who  
534 did not observe a significant variation in alpha diversity along vertical and horizontal river  
535 samples, we noticed a significant decrease in the archaea alpha diversity at t41 (Table S1). This  
536 can be explained by the presence of three OTUs representing 90% of all reads in this sample  
537 (not shown), which belonged to Nitrosopumilaceae and Nitrososphaeraceae families  
538 (Nitrososphaeria class). Nitrososphaeria is the only known ammonia-oxidizing archaea (AOA)  
539 class which accomplishes nitrification in all kinds of environments (Pinto et al. 2020) but has  
540 been specifically found attached to terrestrial soil and freshwater sediments (Sonthiphand et al.  
541 2013; Li et al. 2018). The AOA predominated assemblage at t41 is therefore derived from soil  
542 runoff or sediments from upstream environments or from the resuspension of deep river  
543 sediments, as they became predominant over polluted in-sewer sediments resuspension and  
544 urban runoff-related assemblages that predominated until t38. The last community shift  
545 included a significant enrichment of Thermoplasmata class in samples t44 to t109, that  
546 coincided with the start of the second peak of flow, which occurred due to the release of waters  
547 from the upstream Vinça reservoir (Reoyo-Prats et al. 2017). This class has been associated  
548 with anoxic, sulphide-rich lentic sediments (Fillol et al. 2015; Compte-Port et al. 2017). The  
549 release of water from this reservoir during regular floods is performed via a valve situated at  
550 the bottom of the dam. As the bottom reservoir waters are anoxic (Fovet et al. 2020) and flow  
551 increase at the bottom level of the dam could potentially lead to sediment release as well, both  
552 are potential causes for the increase of Themoplasmata when dam discharges became  
553 predominant at t44.

#### 554 **4.3. Major environmental forces were linked to particle-attached archaeome shifts** 555 **during an extreme event through comprehensive modelling analyses**

556 Among the few papers in the literature that have linked archaeal diversity to environmental  
557 parameters, all addressed the effect of one family of parameters on changes in archaeal  
558 communities, such as nutrients (Herfort et al. 2009; Hu et al. 2016, 2018; Lei et al. 2020; Cao  
559 et al. 2020) or metals (Mahamoud Ahmed et al. 2020; Shen et al. 2021). This is, therefore, the  
560 first study on the Archaea domain where both diversity and a large panoply of physicochemical  
561 parameters (notably nutrients, trace metals, pharmaceuticals, and pesticides) have been  
562 analyzed for the same samples. To analyze such complex datasets, we used a comprehensive

563 analysis as such performed on bacteria (Noyer et al. 2020). On one side, Bokulich *et al.* (2012)  
564 suggested quality-filtering strategies to eliminate artifacts before interpretation of results and  
565 recommended a conservative OTU threshold of 0.005% for bacteria. On the other side, it has  
566 been suggested to use multivariate cut-offs instead of arbitrary thresholds to delineate abundant  
567 versus rare OTUs, as the latest are largely dependent on sequence coverage (Jia et al. 2018).  
568 Furthermore, multivariate cut-offs can be set considering environmental parameters when  
569 available (Gobet et al. 2010). Based on these studies, we designed a strategy with the purpose  
570 to define this cut-off at the point where the constraint-based model which considers OTU  
571 relative abundance (tbRDA model) became significant. The environmental response of the  
572 archaeal community was obtained with a tenfold higher threshold (0.05%) than bacteria  
573 (0.005%, Noyer et al. 2020). This result indicated that archaeal taxa that responded to  
574 environmental pollutants were ten times more abundant than bacteria. Less abundant archaeal  
575 taxa were therefore less crucial than those same bacterial taxa in the response of their respective  
576 communities to environmental parameters. We believe that was the reason why the constraint-  
577 based model obtained when using Bray-Curtis dissimilarity i.e., that considers OTU abundance  
578 only, turned out non-significant for the archaeome (Table 1a) in contrast to the bacteriome. The  
579 other constrained multivariate analyses models that were significant, as well as the constrained  
580 network analyses, gave evidence of two dynamics, ProxyDyn2 and Diuron, as responsible for  
581 major structural diversity shifts observed on riverine particle-attached archaea during the  
582 extreme flood event (Fig. 5 and 6b). These specific dynamics were discharged in the watershed  
583 by CSOs as well as by urban runoff (Reoyo-Prats et al. 2017) from t17 to t38 and represented  
584 several environmental pollutants including pesticides, as well as copper and dissolved  
585 pharmaceutical products and a contaminant, phosphate (see Fig. 1b for further details). These  
586 parameters have been found to affect bacterial communities in freshwater ecosystems, and  
587 metals and nutrients also affect archaeal communities in freshwaters (Hu et al. 2016; Lei et al.  
588 2020; Shen et al. 2021). Nevertheless, to our knowledge, the effect of xenobiotics such as  
589 pesticides or pharmaceutical products on archaeal communities from freshwater ecosystems  
590 has not yet been specifically reported. But, the pesticide glyphosate, for instance, interferes  
591 with the aromatic-acids pathway in microorganisms, including archaea, and alters microbial  
592 communities (van Bruggen et al. 2021). On the other hand, eutrophication by phosphate has  
593 been found to decrease glyphosate degradation by biofilms and increase AMPA accumulation  
594 in surface waters (Carles et al. 2019), what could therefore indirectly affect microbial  
595 communities. The third significant dynamics according to the tbRDA, ProxyDyn1, projected  
596 on axis 2, was mainly linked to the flow peak sample at t38, but axis 2 turned out not significant

597 (Fig. 5). ProxyDyn1 was neither correlated to the significant module of network analyses (Fig.  
598 6).

#### 599 4.4. Key players in the response of the riverine archaeome to multiple stressors

600 One of the major objectives of this study was to identify OTUs which could play a key role in  
601 the archaeal community response to environmental changes derived from the delivery of  
602 xenobiotics into the river by different pollutant sources. OTUs with positive membership to  
603 the significant module from constraint-based network analysis were affiliated with  
604 Euryarchaeota, Halobacterota and Thermoplasmata (Fig. 6a, Table S3.1). These major OTUs  
605 played a significant role in the response of the archaeome to multiple stressors derived from  
606 point sources of pollution, as they were most abundant in samples t17-t23, t37, and t38 (Fig.  
607 6b, Table S3.1) and were linked to ProxyDyn2 and Diuron but not to ProxyDyn1, which is a  
608 proxy for diffuse sources of pollution. The predominant OTU11, affiliated with *Mba. palustre*,  
609 is a species isolated for the first time in peat bogs that has the ability to use secondary alcohols  
610 to produce methane (Zellner et al. 1988; Chaban et al. 2006). *Mbt. smithii* (OTU3) was the  
611 second most abundant key player, which is known to be derived from the human  
612 gastrointestinal tract (Miller et al. 1982; Oliveira et al. 2016) and identified as a potential  
613 indicator of sewage (Johnston et al. 2010; McLellan and Eren 2014). The third most abundant  
614 OTU41 was affiliated with *Msa. concilii*, which is involved in methane production from acetate  
615 (Zwain et al. 2017) and is abundant in-sewer biofilms (Sun et al. 2014). What was striking in  
616 the present study was that other OTUs, which had not yet been linked to CSOs and/or pollutant  
617 inputs in the literature, acted as major OTUs in the response of the archaeome to pollutant  
618 mixtures (Fig. 6a, Table S3.1). Three of them matched Methanobacteria (OTU26) or  
619 Thermoplasmata (OTUs 16 and 19) classes and were also related to methane; and the other  
620 three major OTUs were affiliated to Nanoarchaeia and Bathyarchaeia classes (OTUs 39, 66  
621 and 34). Lastly, several OTUs affiliated to Thermoplasmata and Nitrososphaeria classes, had  
622 a significant negative membership to the module of network analysis linked to ProxyDyn2 and  
623 Diuron (Fig. 6c). These key players were instead linked to samples from the end of the flood  
624 event, from t44 to t109. As evidenced above, they were taxa from allochthonous origins. All  
625 these urban taxa, which were identified as either positively or negatively correlated with major  
626 stressors, could be used as alternative bioindicators for rapid risk assessment of the impact of  
627 multiple stressors on aquatic ecosystems, as proposed for bacteria (McLellan and Eren 2014;  
628 Dila et al. 2018; Noyer et al. 2020).

#### 4.5. Comparison between particle-attached archaeal and bacterial diversity at seasons and along the flood event

Few studies so far have compared archaeal and bacterial structural diversity in lotic ecosystems (Cannon et al. 2017; Hu et al. 2018) and, to the best of our knowledge, the differences in the responses of both domains to seasons have not yet been studied. Fluvial archaeal response to environmental dynamics differed from the bacterial response in three ways. First, the archaeome showed a specific community in summer compared to winter and autumn samples, while bacterial communities from these three seasons clustered together when compared to communities along the flood (Noyer et al. 2020). Second, environmental forces structured the archaeome diversity differently depending on beta diversity distance-based statistical models, particularly when considering qualitative vs. quantitative dissimilarities. These models were not always significant (Table 1), while for bacteria all models were significant. Third, while the bacterial community structured differently at the two multipollution events of this extreme flood, which were derived from CSOs and the flow peak (Reoyo-Prats et al. 2017), archaeal structural shifts could only be interpreted after further statistical modeling of OTU abundances and extreme event dynamics. On the one hand, the archaeal riverine resident communities shifted significantly according to two environmental dynamics only, ProxyDyn2 and Diuron (Fig. 5 and 6). These dynamics were derived from point sources of pollution, such as CSOs, in-sewer sediments resuspension and urban runoff conducted through CSOs. On the other hand, bacteria also responded significantly to other environmental parameters linked to diffuse sources of pollution. Notably, at the highest water discharge at t38 and t41, bacteria showed a specific community that was correlated to ProxyDyn1 and was thus attributed to allochthonous inputs from runoff (Reoyo-Prats et al. 2017). The archaeome shifted at t41 into an anoxic community, most likely related to the resuspension of deep sediments, and was not significantly related to ProxyDyn1 (Fig. 3 and 5) and therefore the flow peak. In conclusion, archaea can help to better understand the origin of watershed sediments and can thus be of interest for quality assessments of suspended matter.

To further understand the different responses of archaea and bacteria domains of life to river contaminants and hydrodynamics, we used a network analysis combined with a module eigengene analysis of bacterial and archaeal taxa best fitted to significant beta diversity models. One remarkable finding was the joint presence of archaea *Mbr. smithii* and *Msa. concilii* with bacteria *Arcobacter cryaerophilus*, *Bacteroides graminisolvens*, *Cloacibacterium normanense* and *Macellibacteroides fermentans* in Module 1, which was significantly correlated with

662 ProxyDyn2 and Diuron. All of these species have already been identified as potential indicators  
663 of human-specific sewage pollution (Dick and Field 2004; Johnston et al. 2010; McLellan and  
664 Eren 2014; McLellan and Roguet 2019) and *A. cryaerophilus* is a known human pathogen  
665 (Collado et al. 2010). While no archaea has yet shown pathogenic effects on humans  
666 (Cavicchioli et al. 2003; Bang and Schmitz 2018), archaea and bacteria can share genes through  
667 horizontal gene transfer, which is particularly enhanced in anaerobic environments (Fuchsman  
668 et al. 2017). Biofilms that develop in urban pipes are anaerobic (Guisasola et al. 2008), and the  
669 co-habitation of archaea with bacterial pathogens in urban systems can increase the risk of  
670 antibiotic resistance gene transfer. Sewers have indeed been identified as reservoirs of  
671 antibiotic-resistance bacteria carried by human pathogens (Millar and Raghavan 2017; Auguet  
672 et al. 2017). Similarly, resistance to pollutants could be enhanced between both domains  
673 through the same mechanisms. Furthermore, the presence of both domains in the same habitat  
674 pointed out to potentially common as well as complementary metabolic and physiological  
675 functions. Another interesting finding that emerged from this analysis was the presence of  
676 archaea together with bacteria OTUs in module 4, which significantly correlated with  $\text{NO}_3^-$   
677 (Fig. 7, Table S3.2). Notably, two Nitrososphaeria class OTUs, known to be dominant in  
678 particle- attached ammonia-oxidizing archaeal communities (Cai et al. 2019; Pinto et al. 2020)  
679 were linked to module 4. Wang *et al.* (2018) also demonstrated a significant influence of  
680 dissolved inorganic nitrogen on the composition of bacterial and archaeal communities along  
681 an urban river. In the present study, the addition of bacterial OTUs in the network analysis  
682 strengthened the importance of nitrates to drive shifts in archaeal assemblages, otherwise  
683 mitigated when archaea were modeled alone, which enhance the interest of studying different  
684 domains of life to better understand environmental drivers of community structure in natural  
685 ecosystems.

## 686 **5. Conclusion**

687 Our study provides the first overview of archaeal community shifts along an extreme storm  
688 event that led to multiple pollutions in a typical coastal Mediterranean watercourse. Shifts were  
689 also compared with changes in archaeal diversity during three seasons. Archaea from the Têt  
690 river showed a specific community in summer compared to winter and autumn samples, and a  
691 higher alpha diversity and lower evenness could be observed in this river compared to other,  
692 yet less-thorough studies on riverine archaeal communities. Further studies on the spatio-  
693 temporal shifts in archaeal assemblages in these ecosystems are therefore urgently needed to

694 better understand seasonal shifts as well as their ecological diversity. For the first time, a  
695 comparison of the response of archaea alone and together with bacteria in a fluvial ecosystem  
696 has shed light on the similarities and differences in their responses to seasons and when facing  
697 multiple stressors derived from an extreme event. The fluvial bacteriome and archaeome did  
698 not respond in the same way to environmental forces. Extreme events were stronger at  
699 structuring bacterial communities than seasons, while the opposite was observed in archaeal  
700 communities. In contrast to bacteria, which responded quickly and significantly to both sewage  
701 overflow and river hydrodynamics and associated environmental parameter changes, the  
702 archaeal community shifted in response to multipollution derived from point sources and from  
703 the resuspension of deep anoxic sediments but not so clearly at the river flow peak. Archaeal  
704 taxa already known as urban-specific, as well as new archaea, mainly methane-related and  
705 never identified as urban-specific taxa, predominated assemblages during multiple stress  
706 events and were confirmed through statistical modeling of archaeal alone and together with  
707 bacteria. These taxa could be used as bioindicators of point sources of pollution. Our results  
708 highlight fluvial archaea, seldom considered as bioindicators of water quality, could provide  
709 a rapid risk assessment of multiple pollutants in aquatic ecosystems, as is the case for bacteria.  
710 Furthermore, a better understanding of parallel shifts in assemblages from both domains of life  
711 when confronted with multiple stressors could help to improve how urban watersheds are  
712 monitored and would thus be extremely helpful in the management of pollution risk.

713

#### 714 **Data Availability**

715 Sequencing data are deposited on NCBI under BioProject ID PRJNA602803.

716

#### 717 **Supplementary Information**

718 Additional Supporting Information may be found in the online version of this article at the  
719 publisher's website.

720

#### 721 **Supplementary Information S1**

722 **Table S1.** Alpha diversity indices at the Têt river with Kruskal-Wallis test results and graphical  
723 representation for each index.

724

#### 725 **Supplementary Information S2**

726 **Fig. S2.1.** Beta diversity based on additional dissimilarities.

727 **Fig. S2.2.** Jaccard, Unifrac and Weighted-Unifrac distance-based RDA triplot.

728 **Supplementary Information S3**

729 **Table S3.1.** Key player significant archaeal OTUs in module eigengene analysis significantly  
730 related to environmental dynamics and graphical representation of their total reads along time.

731 **Table S3.2.** Key player significant bacterial or archaea OTUs in modules derived from module  
732 eigengene analysis significantly related to environmental dynamics.

733

734 **Statements & Declarations**

735 **Funding**

736 This work was supported by scholarships from Ecole Doctorale Energie et Environnement (E2-  
737 UPVD) and from Region Occitanie to MN (n. 2017-19-ED.305). Supporting projects were:  
738 DEBiMicro (2013 BQR CEFREM to CP), StepBiodiv (2015-2017 VEOLIA-Eau Perpignan to  
739 OV); and DEBi2Micro (2016-17 EC2CO CNRS INSU to CP).

740

741 **Competing Interests**

742 The authors have no relevant financial or non-financial interests to disclose.

743

744 **Contributions**

745 Megane Noyer and Carmen Palacios contributed to conception and design of the study,  
746 organized the database, performed the statistical analyses and wrote the first draft of the  
747 manuscript. Maria Bernard helped with metabarcoding analyses. All authors contributed to  
748 manuscript revision, read and approved the submitted version.

749

750 **Ethical Approval**

751 Not applicable.

752

753 **Consent to Participate**

754 All authors are informed and agree to the study.

755

756 **Consent to Publish**

757 The authors declare no competing interests.

758 **References**

- 759 Adam PS, Borrel G, Brochier-Armanet C, Gribaldo S (2017) The growing tree of Archaea:  
760 new perspectives on their diversity, evolution and ecology. *The ISME Journal* 11:2407–  
761 2425. <https://doi.org/10.1038/ismej.2017.122>
- 762 Amalfitano S, Corno G, Eckert E, et al (2017) Tracing particulate matter and associated  
763 microorganisms in freshwaters. *Hydrobiologia* 800:145–154.  
764 <https://doi.org/10.1007/s10750-017-3260-x>
- 765 Ashley RM, Wotherspoon DJJ, Coghlan BP, McGregor I (1992) The Erosion and Movement  
766 of Sediments and Associated Pollutants in Combined Sewers. *Water Science and*  
767 *Technology* 25:101–114. <https://doi.org/10.2166/wst.1992.0184>
- 768 Auguet J-C, Barberan A, Casamayor EO (2010) Global ecological patterns in uncultured  
769 Archaea. *The ISME Journal* 4:182–190. <https://doi.org/10.1038/ismej.2009.109>
- 770 Auguet O, Pijuan M, Borrego CM, et al (2017) Sewers as potential reservoirs of antibiotic  
771 resistance. *Science of The Total Environment* 605–606:1047–1054.  
772 <https://doi.org/10.1016/j.scitotenv.2017.06.153>
- 773 Bang C, Schmitz RA (2018) Archaea: forgotten players in the microbiome. *Emerging Topics*  
774 *in Life Sciences* 2:459–468. <https://doi.org/10.1042/ETLS20180035>
- 775 Blanchet J, Molinié G, Touati J (2016) Spatial analysis of trend in extreme daily rainfall in  
776 southern France. *Climate Dynamics* 51:799–812. <https://doi.org/10.1007/s00382-016-3122-7>
- 778 Bokulich NA, Subramanian S, Faith JJ, et al (2012) Quality-filtering vastly improves diversity  
779 estimates from Illumina amplicon sequencing. *Nature Methods* 10:57–59.  
780 <https://doi.org/10.1038/nmeth.2276>
- 781 Borrego C, Sabater S, Proia L (2020) Lifestyle preferences drive the structure and diversity of  
782 bacterial and archaeal communities in a small riverine reservoir. *Scientific Reports* 10:.  
783 <https://doi.org/10.1038/s41598-020-67774-0>
- 784 Cai X, Yao L, Hu Y, et al (2019) Particle-attached microorganism oxidation of ammonia in a  
785 hypereutrophic urban river. *Journal of Basic Microbiology* 59:511–524.  
786 <https://doi.org/10.1002/jobm.201800599>
- 787 Cameron ES, Schmidt PJ, Tremblay BJ-M, et al (2021) Enhancing diversity analysis by  
788 repeatedly rarefying next generation sequencing data describing microbial  
789 communities. *Sci Rep* 11:22302. <https://doi.org/10.1038/s41598-021-01636-1>
- 790 Cannon MV, Craine J, Hester J, et al (2017) Dynamic microbial populations along the  
791 Cuyahoga River. *PLOS ONE* 12:e0186290.  
792 <https://doi.org/10.1371/journal.pone.0186290>
- 793 Cao X, Wang Y, Xu Y, et al (2020) Adaptive variations of sediment microbial communities  
794 and indication of fecal-associated bacteria to nutrients in a regulated urban river. *Water*  
795 12:1344. <https://doi.org/10.3390/w12051344>

- 796 Carles L, Gardon H, Joseph L, et al (2019) Meta-analysis of glyphosate contamination in  
797 surface waters and dissipation by biofilms. *Environment International* 124:284–293.  
798 <https://doi.org/10.1016/j.envint.2018.12.064>  
799
- 800 Casamayor EO, Borrego CM (2009) Archaea in inland waters. In *Encyclopedia of Inland*  
801 *Waters* Likens, G (ed) Oxford, UK: Academic Press, Elsevier
- 802 Castelle CJ, Wrighton KC, Thomas BC, et al (2015) Genomic expansion of domain archaea  
803 highlights roles for organisms from new phyla in anaerobic carbon cycling. *Current*  
804 *Biology* 25:690–701. <https://doi.org/10.1016/j.cub.2015.01.014>
- 805 Cavicchioli R, Curmi PMG, Saunders N, Thomas T (2003) Pathogenic archaea: do they exist?  
806 *BioEssays* 25:1119–1128. <https://doi.org/10.1002/bies.10354>
- 807 Chaban B, Ng SYM, Jarrell KF (2006) Archaeal habitats — from the extreme to the ordinary.  
808 *Canadian Journal of Microbiology* 52:73–116. <https://doi.org/10.1139/w05-147>
- 809 Clarke KR (1993) Non-parametric multivariate analyses of changes in community structure.  
810 *Austral Ecology* 18:117–143. <https://doi.org/10.1111/j.1442-9993.1993.tb00438.x>
- 811 Collado L, Kasimir G, Perez U, et al (2010) Occurrence and diversity of *Arcobacter* spp. along  
812 the Llobregat River catchment, at sewage effluents and in a drinking water treatment  
813 plant. *Water Research* 44:3696–3702. <https://doi.org/10.1016/j.watres.2010.04.002>
- 814 Compte-Port S, Subirats J, Fillol M, et al (2017) Abundance and co-distribution of widespread  
815 marine archaeal lineages in surface sediments of freshwater water bodies across the  
816 iberian peninsula. *Microb Ecol* 74:776–787. [https://doi.org/10.1007/s00248-017-0989-](https://doi.org/10.1007/s00248-017-0989-8)  
817 8
- 818 Conseil Général des Pyrénées Orientales (CG66). Suivi de la qualité des cours d'eau du bassin  
819 versant de la Têt Année - Rapport final année 2012.
- 820 Conseil Général des Pyrénées Orientales (CG66). Suivi de la qualité des cours d'eau du bassin  
821 versant de la Têt Année - Rapport final année 2009.
- 822 Cowling RM, Ojeda F, Lamont BB, et al (2005) Rainfall reliability, a neglected factor in  
823 explaining convergence and divergence of plant traits in fire-prone mediterranean-  
824 climate ecosystems: Rainfall reliability in mediterranean-climate ecosystems. *Global*  
825 *Ecology and Biogeography* 14:509–519. [https://doi.org/10.1111/j.1466-](https://doi.org/10.1111/j.1466-822X.2005.00166.x)  
826 822X.2005.00166.x
- 827 Crump BC, Baross JA (2000) Archaeaplankton in the Columbia River, its estuary and the  
828 adjacent coastal ocean, USA. *FEMS Microbiology Ecology* 31:231–239.  
829 <https://doi.org/10.1111/j.1574-6941.2000.tb00688.x>
- 830 Deng Y, Jiang Y-H, Yang Y, et al (2012) Molecular ecological network analyses. *BMC*  
831 *Bioinformatics* 13:113. <https://doi.org/10.1186/1471-2105-13-113>
- 832 Dick LK, Field KG (2004) Rapid estimation of numbers of fecal Bacteroidetes by use of a  
833 quantitative PCR assay for 16S rRNA genes. *Applied and Environmental Microbiology*  
834 70:5695–5697. <https://doi.org/10.1128/AEM.70.9.5695-5697.2004>

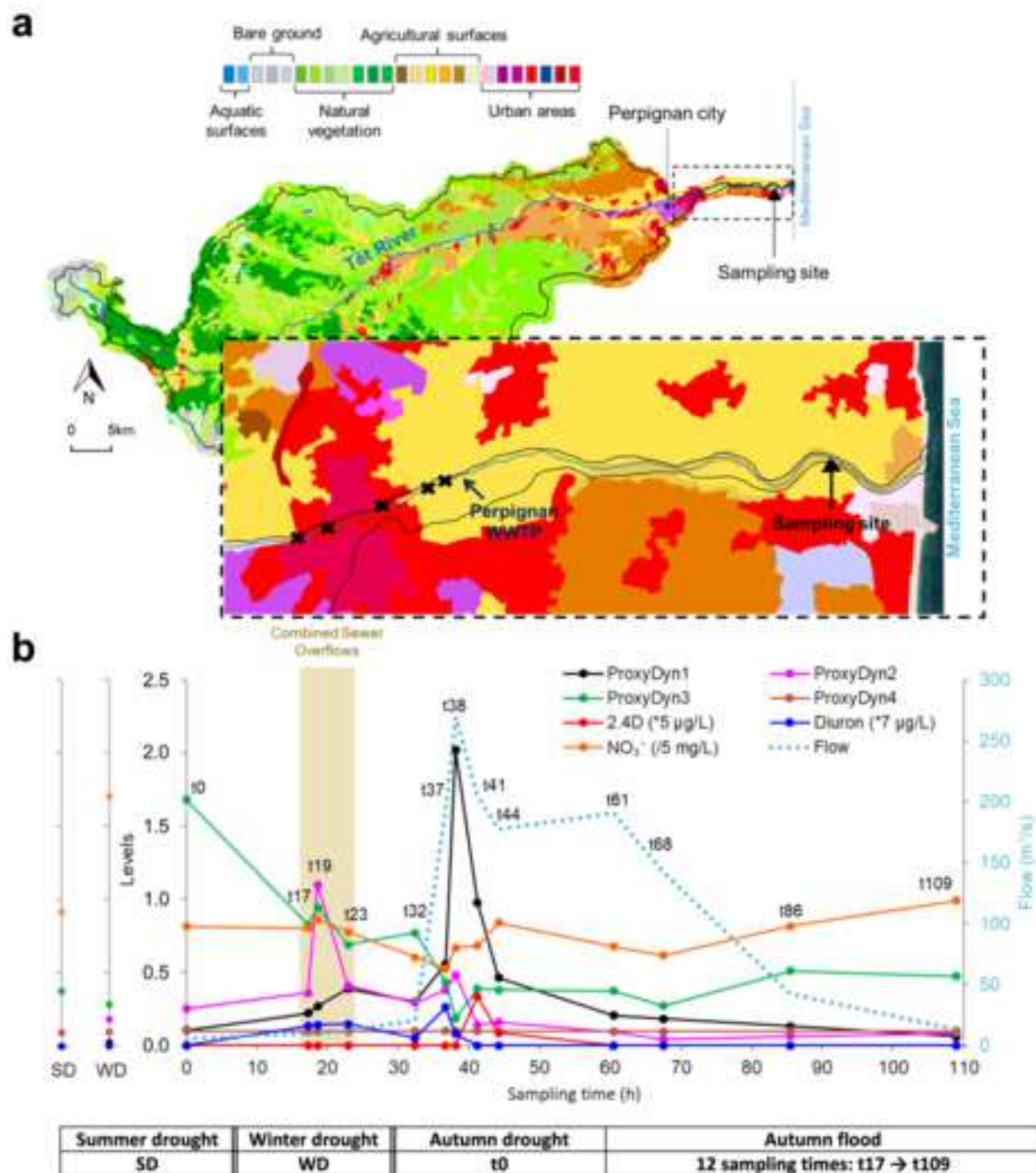
- 835 Dila DK, Corsi SR, Lenaker PL, et al (2018) Patterns of host-associated fecal indicators driven  
836 by hydrology, precipitation, and land use attributes in great lakes watersheds.  
837 *Environmental Science & Technology*. <https://doi.org/10.1021/acs.est.8b01945>
- 838 Dumas C, Ludwig W, Aubert D, et al (2015) Riverine transfer of anthropogenic and natural  
839 trace metals to the Gulf of Lions (NW Mediterranean Sea). *Applied Geochemistry*  
840 58:14–25. <https://doi.org/10.1016/j.apgeochem.2015.02.017>
- 841 Escudié F, Auer L, Bernard M, et al (2018) FROGS: Find, Rapidly, OTUs with Galaxy  
842 Solution. *Bioinformatics* 34:1287–1294. <https://doi.org/10.1093/bioinformatics/btx791>
- 843 Faure D, Bonin P, Duran R, the Microbial Ecology EC2CO consortium (2015) Environmental  
844 microbiology as a mosaic of explored ecosystems and issues. *Environ Sci Pollut Res*  
845 22:13577–13598. <https://doi.org/10.1007/s11356-015-5164-5>
- 846 Fillol M, Sànchez-Melsió A, Gich F, M. Borrego C (2015) Diversity of Miscellaneous  
847 Crenarchaeotic Group archaea in freshwater karstic lakes and their segregation between  
848 planktonic and sediment habitats. *FEMS Microbiology Ecology* 91:.  
849 <https://doi.org/10.1093/femsec/fiv020>
- 850 Fovet O, Ndom M, Crave A, Pannard A (2020) Influence of dams on river water- quality  
851 signatures at event and seasonal scales: The Sélune River (France) case study. *River*  
852 *Research and Applications* 36:1267-1278
- 853 Fuchsman CA, Collins RE, Rocap G, Brazelton WJ (2017) Effect of the environment on  
854 horizontal gene transfer between bacteria and archaea. *PeerJ* 5:e3865.  
855 <https://doi.org/10.7717/peerj.3865>
- 856 Garcia-Esteves J, Ludwig W, Kerhervé P, et al (2007) Predicting the impact of land use on the  
857 major element and nutrient fluxes in coastal Mediterranean rivers: The case of the Têt  
858 River (Southern France). *Applied Geochemistry* 22:230–248.  
859 <https://doi.org/10.1016/j.apgeochem.2006.09.013>
- 860 Gobet A, Boetius A, Ramette A (2014) Ecological coherence of diversity patterns derived from  
861 classical fingerprinting and Next Generation Sequencing techniques. *Environmental*  
862 *Microbiology* 16:2672–2681. <https://doi.org/10.1111/1462-2920.12308>
- 863 Gobet A, Quince C, Ramette A (2010) Multivariate Cutoff Level Analysis (MultiCoLA) of  
864 large community data sets. *Nucleic Acids Research* 38:e155–e155.  
865 <https://doi.org/10.1093/nar/gkq545>
- 866 Guisasola A, de Haas D, Keller J, Yuan Z (2008) Methane formation in sewer systems. *Water*  
867 *Research* 42:1421–1430. <https://doi.org/10.1016/j.watres.2007.10.014>
- 868 Herfort L, Kim J, Coolen M, et al (2009) Diversity of Archaea and detection of crenarchaeotal  
869 amoA genes in the rivers Rhine and Têt. *Aquatic Microbial Ecology* 55:189–201.  
870 <https://doi.org/10.3354/ame01294>
- 871 Hu A, Wang H, Li J, et al (2016) Archaeal community in a human-disturbed watershed in  
872 southeast China: diversity, distribution, and responses to environmental changes. *Appl*  
873 *Microbiol Biotechnol* 100:4685–4698. <https://doi.org/10.1007/s00253-016-7318-x>

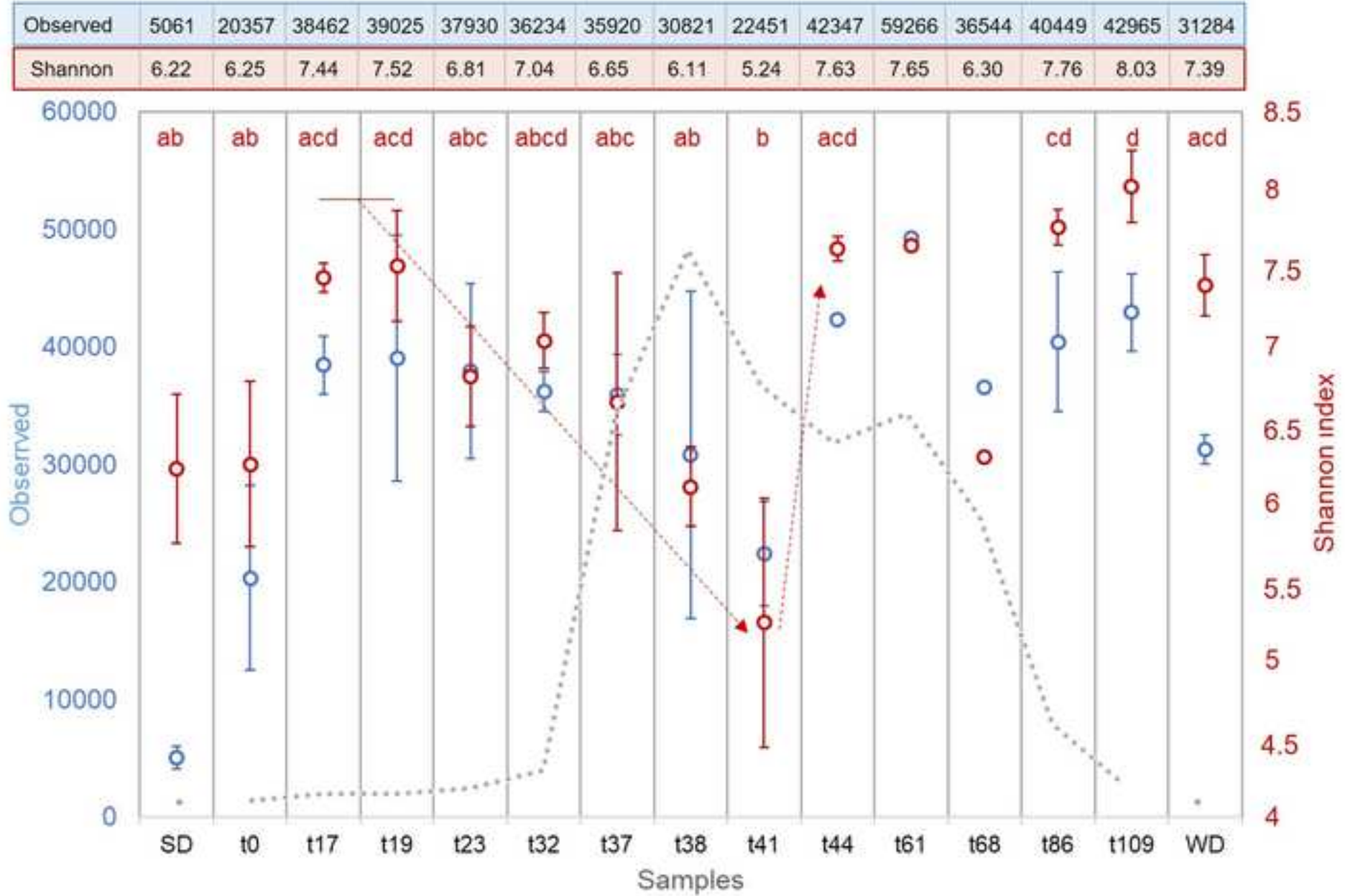
- 874 Hu Y, Cai J, Bai C, et al (2018) Contrasting patterns of the bacterial and archaeal communities  
875 in a high-elevation river in northwestern China. *Journal of Microbiology* 56:104–112.  
876 <https://doi.org/10.1007/s12275-018-7244-y>
- 877 Jia X, Dini-Andreote F, Falcão Salles J (2018) Community Assembly Processes of the  
878 Microbial Rare Biosphere. *Trends in Microbiology* 26:738–747.  
879 <https://doi.org/10.1016/j.tim.2018.02.011>
- 880 Johnston C, Ufnar JA, Griffith JF, et al (2010) A real-time qPCR assay for the detection of the  
881 *nifH* gene of *Methanobrevibacter smithii*, a potential indicator of sewage pollution: A  
882 qPCR assay for detecting *Methanobrevibacter smithii*. *Journal of Applied*  
883 *Microbiology* 109:1946–1956. <https://doi.org/10.1111/j.1365-2672.2010.04824.x>
- 884 Joye SB (2012) A piece of the methane puzzle. *Nature* 491:538–539.  
885 <https://doi.org/10.1038/nature11749>  
886
- 887 Langfelder P, Horvath S (2007) Eigengene networks for studying the relationships between  
888 co-expression modules. *BMC Systems Biology* 1, 54:. [https://doi.org/10.1186/1752-](https://doi.org/10.1186/1752-0509-1-54)  
889 [0509-1-54](https://doi.org/10.1186/1752-0509-1-54)
- 890 Legendre P, Gallagher ED (2001) Ecologically meaningful transformations for ordination of  
891 species data. *Oecologia* 129:271–280. <https://doi.org/10.1007/s004420100716>
- 892 Legendre P, Legendre L (2012) *Numerical Ecology*. Elsevier. ISBN: 978-0-444-53869-7  
893
- 894 Lei M, Li Y, Zhang W, et al (2020) Identifying ecological processes driving vertical and  
895 horizontal archaeal community assemblages in a contaminated urban river.  
896 *Chemosphere* 245:125615. <https://doi.org/10.1016/j.chemosphere.2019.125615>
- 897 Li M, Wei G, Shi W, et al (2018) Distinct distribution patterns of ammonia-oxidizing archaea  
898 and bacteria in sediment and water column of the Yellow River estuary. *Sci Rep* 8:1584.  
899 <https://doi.org/10.1038/s41598-018-20044-6>
- 900 Magurran AE (2004) *Measuring biological diversity*. Blackwell Pub, Malden, Ma
- 901 Mahamoud Ahmed A, Tardy V, Bonnineau C, et al (2020) Changes in sediment microbial  
902 diversity following chronic copper-exposure induce community copper-tolerance  
903 without increasing sensitivity to arsenic. *Journal of Hazardous Materials* 391:122197.  
904 <https://doi.org/10.1016/j.jhazmat.2020.122197>
- 905 McLellan SL, Eren AM (2014) Discovering new indicators of fecal pollution. *Trends in*  
906 *Microbiology* 22:697–706. <https://doi.org/10.1016/j.tim.2014.08.002>
- 907 McLellan SL, Roguet A (2019) The unexpected habitat in sewer pipes for the propagation of  
908 microbial communities and their imprint on urban waters. *Current Opinion in*  
909 *Biotechnology* 57:34–41. <https://doi.org/10.1016/j.copbio.2018.12.010>
- 910 McMurdie PJ, Holmes S (2013) phyloseq: An R package for reproducible interactive analysis  
911 and graphics of microbiome census data. *PLoS ONE* 8(4):e61217.  
912 <https://doi.org/10.1371/journal.pone.0061217>

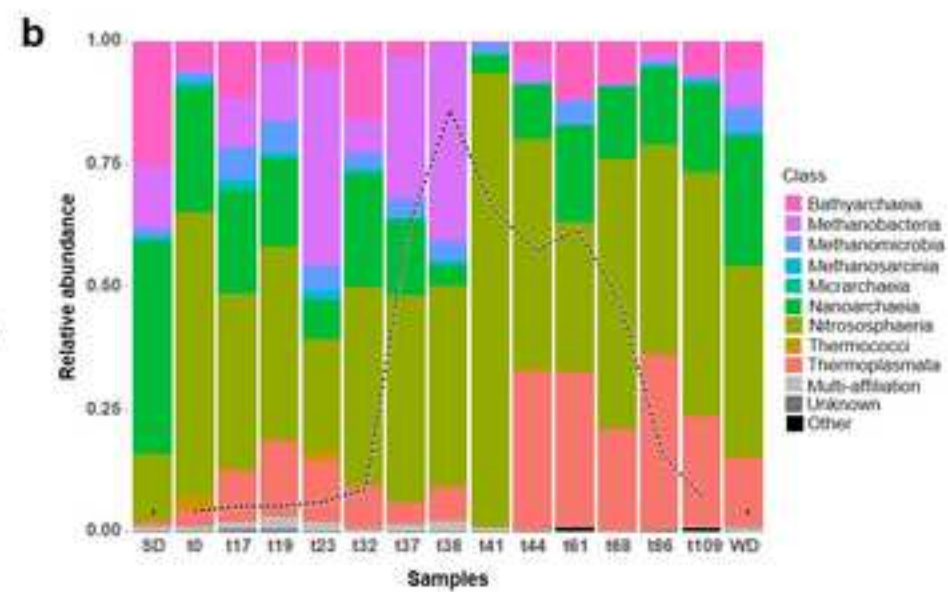
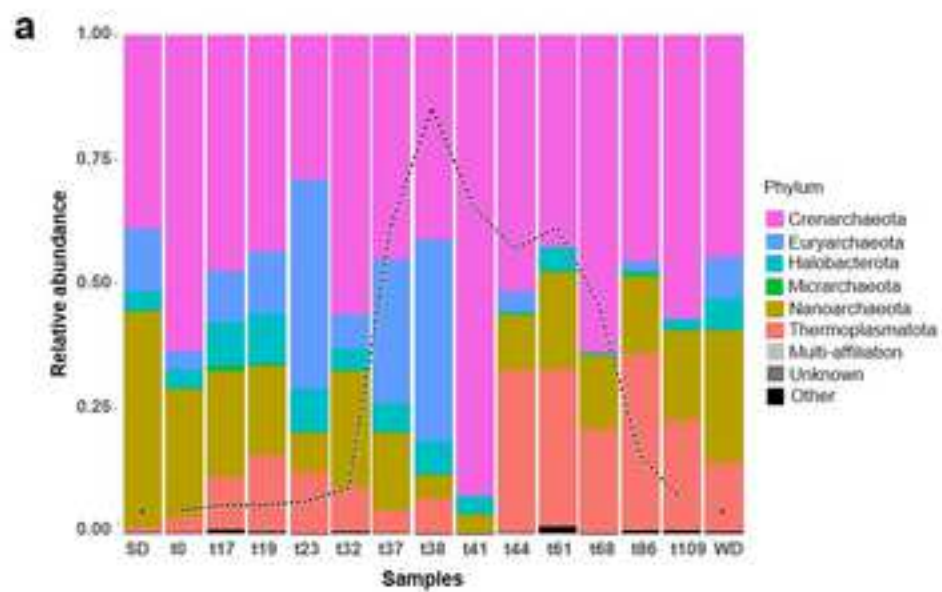
- 913 McMurdie PJ, Holmes S (2014) Waste not, want not: why rarefying microbiome data is  
914 inadmissible. PLoS Comput Biol 10:e1003531.  
915 <https://doi.org/10.1371/journal.pcbi.1003531>
- 916 Millar JA, Raghavan R (2017) Accumulation and expression of multiple antibiotic resistance  
917 genes in *Arcobacter cryaerophilus* that thrives in sewage. PeerJ 5:e3269.  
918 <https://doi.org/10.7717/peerj.3269>
- 919 Miller TL, Wolin MJ, Macario AJ (1982) Isolation of *Methanobrevibacter smithii* from Human  
920 Feces. Applied and Environmental Microbiology 43:227–232
- 921 Newman MEJ (2004) Fast algorithm for detecting community structure in networks. Physical  
922 Review E 69:. <https://doi.org/10.1103/PhysRevE.69.066133>
- 923 Noyer M, Reoyo-Prats B, Aubert D, et al (2020) Particle-attached riverine bacteriome shifts in  
924 a pollutant-resistant and pathogenic community during a Mediterranean extreme storm  
925 event. Science of The Total Environment 139047.  
926 <https://doi.org/10.1016/j.scitotenv.2020.139047>
- 927 Offre P, Spang A, Schleper C (2013) Archaea in biogeochemical cycles. Annual Review of  
928 Microbiology 67:437–457. <https://doi.org/10.1146/annurev-micro-092412-155614>
- 929 Oksanen J, Blanchet FG, Friendly M, et al (2018) Vegan: community ecology package. R  
930 package version 2.5-3.
- 931 Oliveira SS, Sorgine MHF, Bianco K, et al (2016) Detection of human fecal contamination by  
932 nifH gene quantification of marine waters in the coastal beaches of Rio de Janeiro,  
933 Brazil. Environ Sci Pollut Res 23:25210–25217. <https://doi.org/10.1007/s11356-016-7737-3>
- 935 Osorio V, Marcé R, Pérez S, et al (2012) Occurrence and modeling of pharmaceuticals on a  
936 sewage-impacted Mediterranean river and their dynamics under different hydrological  
937 conditions. Science of The Total Environment 440:3–13.  
938 <https://doi.org/10.1016/j.scitotenv.2012.08.040>
- 939 Oursel B, Garnier C, Zebracki M, et al (2014) Flood inputs in a Mediterranean coastal zone  
940 impacted by a large urban area: Dynamic and fate of trace metals. Marine Chemistry  
941 167:44–56. <https://doi.org/10.1016/j.marchem.2014.08.005>
- 942 Pinto OHB, Silva TF, Vizzotto CS, et al (2020) Genome-resolved metagenomics analysis  
943 provides insights into the ecological role of Thaumarchaeota in the Amazon River and  
944 its plume. BMC Microbiology 20:. <https://doi.org/10.1186/s12866-020-1698-x>
- 945 Pons P, Latapy M (2005) Computing Communities in Large Networks Using Random Walks.  
946 In: Yolum pInar, Güngör T, Gürgen F, Özturan C (eds) Computer and Information  
947 Sciences - ISCIS 2005. Springer Berlin Heidelberg, Berlin, Heidelberg, pp 284–293
- 948 R Core Team (2018) R: A language and environment for statistical computing. R Foundation  
949 for Statistical Computing, Vienna
- 950 Reoyo-Prats B, Aubert D, Menniti C, et al (2017) Multicontamination phenomena occur more  
951 often than expected in Mediterranean coastal watercourses: Study case of the Têt River

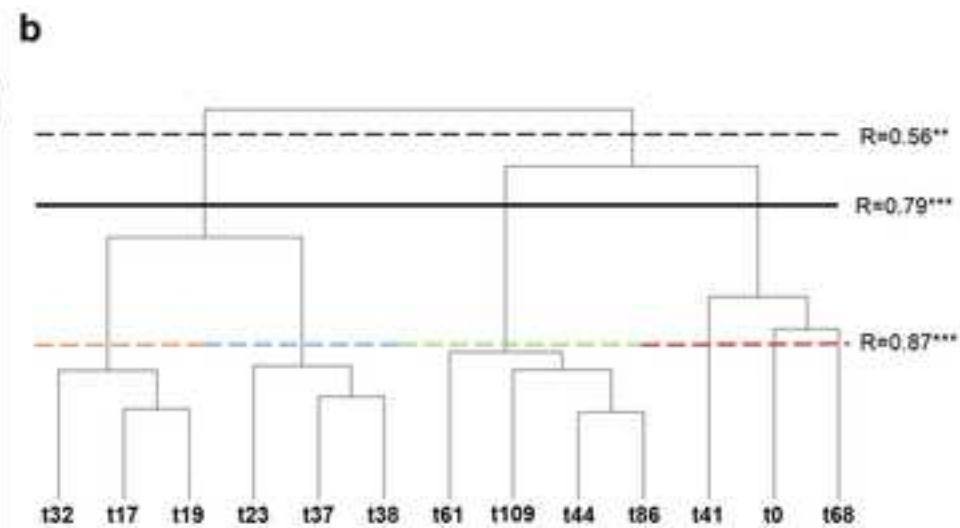
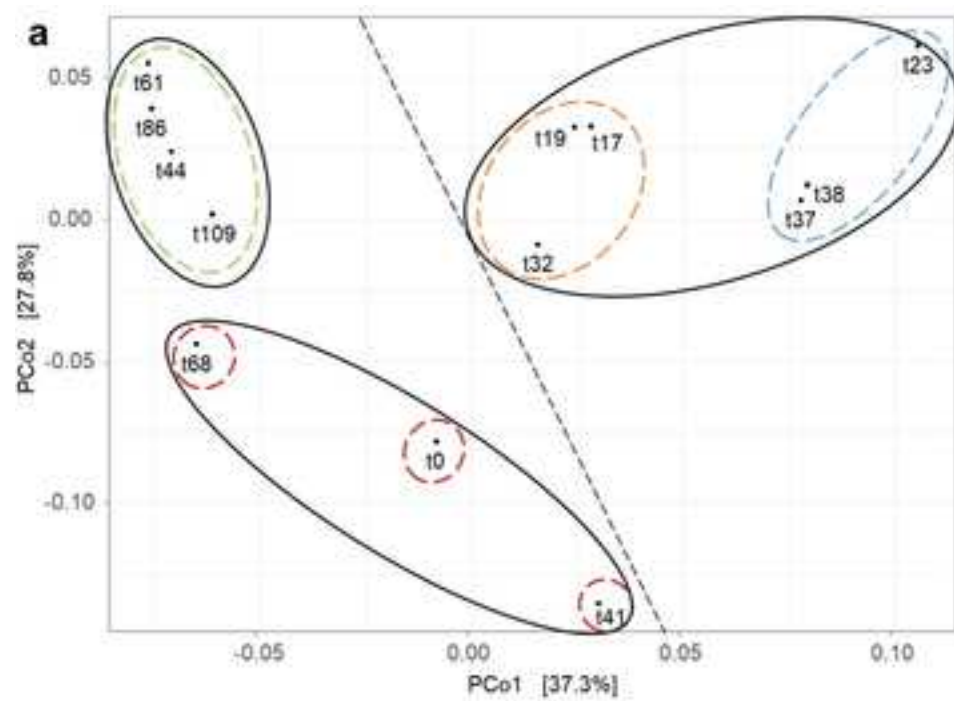
- 952 (France). *Science of The Total Environment* 579:10–21.  
953 <https://doi.org/10.1016/j.scitotenv.2016.11.019>
- 954 Reoyo-Prats B, Aubert D, Sellier A, et al (2018) Dynamics and sources of pharmaceutically  
955 active compounds in a coastal Mediterranean river during heavy rains. *Environmental*  
956 *Science and Pollution Research* 25:6107–6121. [https://doi.org/10.1007/s11356-017-](https://doi.org/10.1007/s11356-017-0880-7)  
957 [0880-7](https://doi.org/10.1007/s11356-017-0880-7)
- 958 Rognes T, Flouri T, Nichols B, et al (2016) VSEARCH: a versatile open source tool for  
959 metagenomics. *PeerJ* 4:e2584. <https://doi.org/10.7717/peerj.2584>
- 960 Samson R, Shah M, Yadav R, et al (2019) Metagenomic insights to understand transient  
961 influence of Yamuna River on taxonomic and functional aspects of bacterial and  
962 archaeal communities of River Ganges. *Science of The Total Environment* 674:288–  
963 299. <https://doi.org/10.1016/j.scitotenv.2019.04.166>
- 964 Shannon P, Markiel A, Ozier O, et al (2003) Cytoscape: a software environment for integrated  
965 models of biomolecular interaction networks. *Genome Research* 13:2498–2504.  
966 <https://doi.org/10.1101/gr.1239303>
- 967 Shen C, Zhao J, Xie G, et al (2021) Identifying microbial distribution drivers of archaeal  
968 community in sediments from a black-odorous urban river—a case study of the Zhang  
969 River Basin. *Water* 13:1545. <https://doi.org/10.3390/w13111545>
- 970 Sonthiphand P, Cejudo E, Schiff SL, Neufeld JD (2013) Wastewater effluent impacts  
971 ammonia-oxidizing prokaryotes of the grand river, Canada. *Appl Environ Microbiol*  
972 79:7454–7465. <https://doi.org/10.1128/AEM.02202-13>
- 973 Sun J, Hu S, Sharma KR, et al (2014) Stratified microbial structure and activity in sulfide- and  
974 methane-producing anaerobic sewer biofilms. *Appl Environ Microbiol* 80:7042–7052.  
975 <https://doi.org/10.1128/AEM.02146-14>
- 976 Tao J, Meng D, Qin C, et al (2018) Integrated network analysis reveals the importance of  
977 microbial interactions for maize growth. *Appl Microbiol Biotechnol* 102:3805–3818.  
978 <https://doi.org/10.1007/s00253-018-8837-4>
- 979 ter Braak CJF (1988) Unimodal models to relate species to environment. *Agricultural*  
980 *Mathematics Group*, 1987. *Biometrics* 44:631–632
- 981 Turner A, Millward GE (2002) Suspended particles: their role in estuarine biogeochemical  
982 cycles. *Estuarine, Coastal and Shelf Science* 55:857–883.  
983 <https://doi.org/10.1006/ecss.2002.1033>
- 984 van Bruggen AHC, Finckh MR, He M, et al (2021) Indirect Effects of the Herbicide Glyphosate  
985 on Plant, Animal and Human Health Through its Effects on Microbial Communities.  
986 *Front Environ Sci* 9:763917. <https://doi.org/10.3389/fenvs.2021.763917>  
987
- 988 Walters KE, Martiny JBH (2020) Alpha-, beta-, and gamma-diversity of bacteria varies across  
989 habitats. *PLoS ONE* 15:e0233872. <https://doi.org/10.1371/journal.pone.0233872>

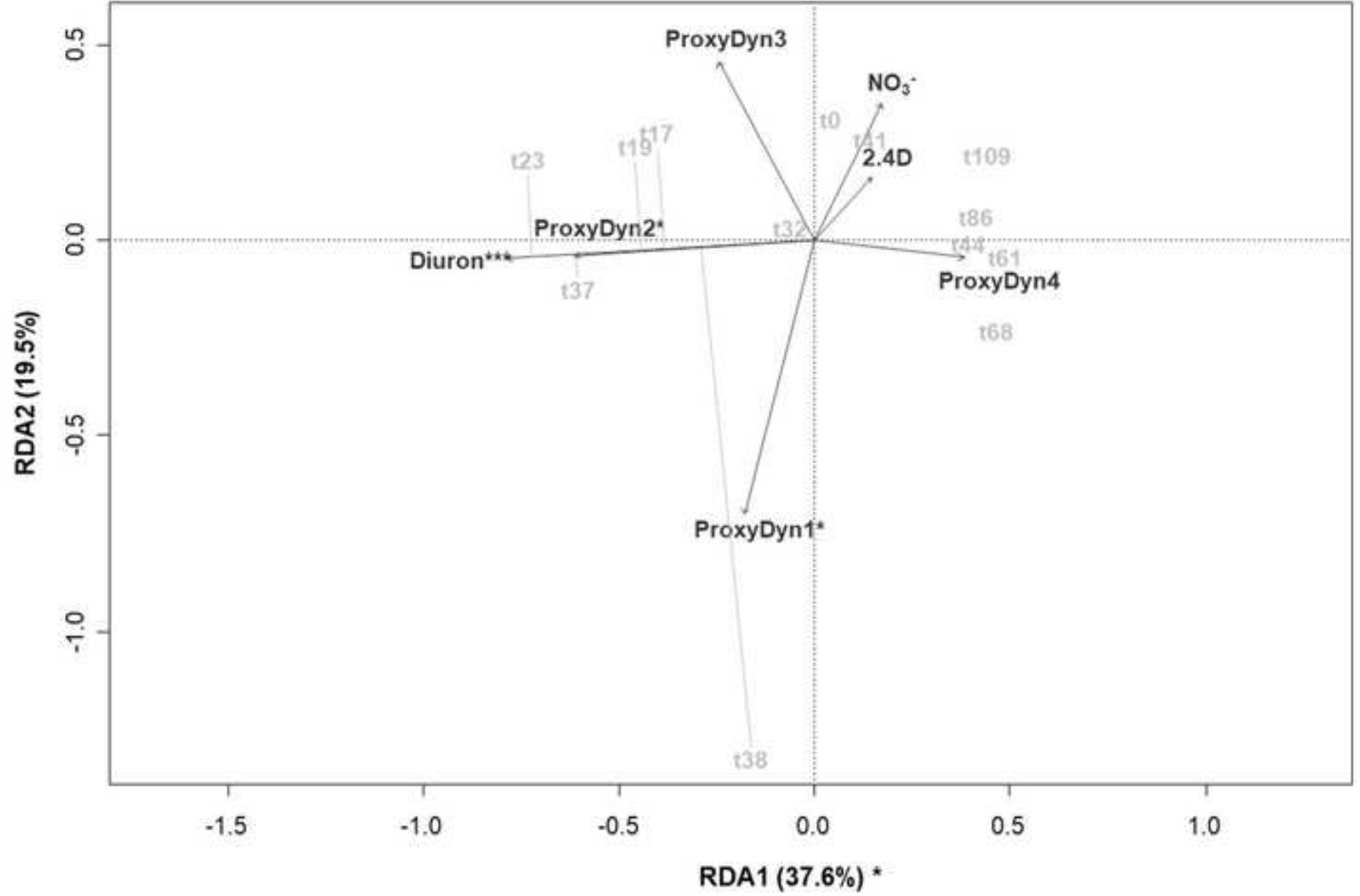
- 990 Wang L, Zhang J, Li H, et al (2018) Shift in the microbial community composition of surface  
991 water and sediment along an urban river. *Science of The Total Environment* 627:600–  
992 612. <https://doi.org/10.1016/j.scitotenv.2018.01.203>
- 993 Woese CR, Fox GE (1977) Phylogenetic structure of the prokaryotic domain: The primary  
994 kingdoms. *Proceedings of the National Academy of Sciences* 74:5088–5090.  
995 <https://doi.org/10.1073/pnas.74.11.5088>
- 996 Woese CR, Magrum LJ, Fox GE (1978) Archaeobacteria. *Journal of Molecular Evolution*  
997 11:245–252. <https://doi.org/10.1007/BF01734485>
- 998 Zeglin LH (2015) Stream microbial diversity in response to environmental changes: review  
999 and synthesis of existing research. *Frontiers in Microbiology* 6:454:  
1000 <https://doi.org/10.3389/fmicb.2015.00454>
- 1001 Zellner G, Bleicher K, Braun E, et al (1988) Characterization of a new mesophilic, secondary  
1002 alcohol-utilizing methanogen, *Methanobacterium palustre* spec. nov. from a peat bog.  
1003 *Archives of Microbiology* 151:1–9. <https://doi.org/10.1007/BF00444660>
- 1004 Zinger L, Gobet A, Pommier T (2012) Two decades of describing the unseen majority of  
1005 aquatic microbial diversity: Sequencing aquatic microbial diversity. *Molecular Ecology*  
1006 21:1878–1896. <https://doi.org/10.1111/j.1365-294X.2011.05362.x>
- 1007 Zwain HM, Aziz HA, Ng WJ, Dahlan I (2017) Performance and microbial community analysis  
1008 in a modified anaerobic inclining-baffled reactor treating recycled paper mill effluent.  
1009 *Environmental Science and Pollution Research* 24:13012–13024.  
1010 <https://doi.org/10.1007/s11356-017-8804-0>
- 1011

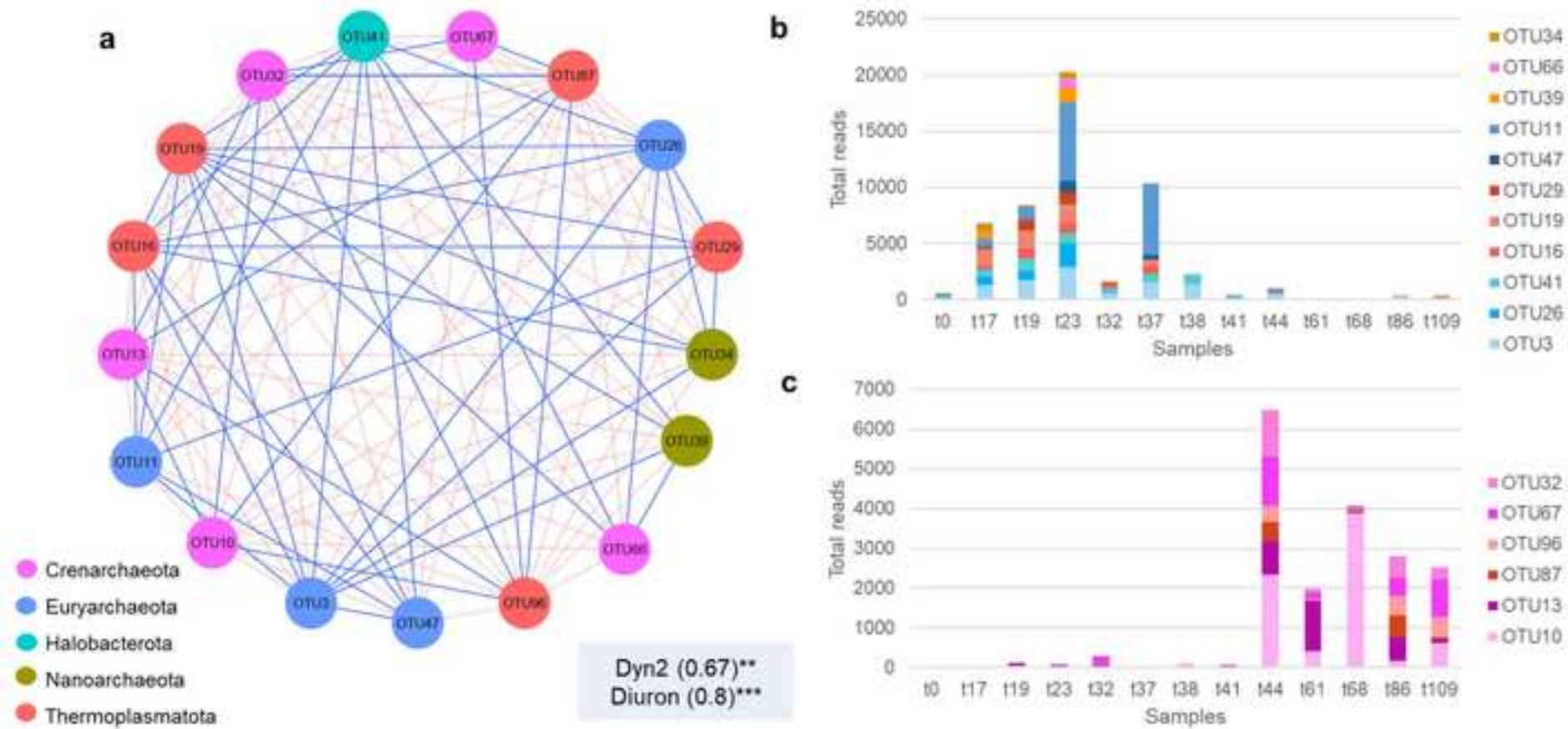












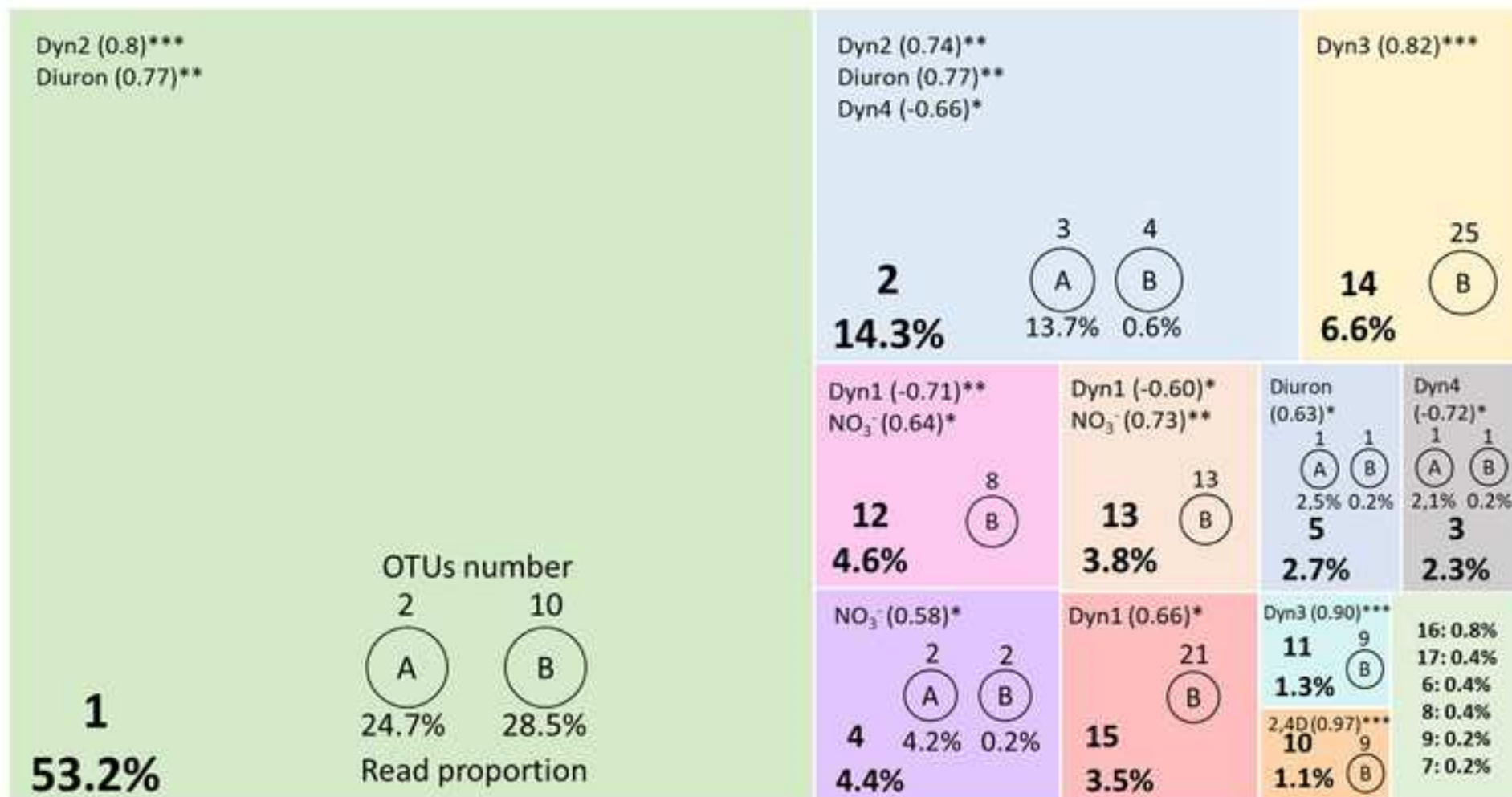


**Fig. 1** Têt River archaeome sampling sites and environmental parameters measured in the same samples. (a) Watershed of the river with sampling site (black arrow), located after wastewater treatment plan (WWTP) of the city of Perpignan, combined sewers (black crosses) and water reservoirs indicated as grey rectangles (adapted from Reoyo-Prats *et al.* 2017). (b) Environmental parameter dynamics in the Têt River at different seasons and along an autumn flood. For sample names, see table below figure. Autumn sample names are followed by a number that indicates the sampling time in hours after t<sub>0</sub>, which was sampled at autumn basal level water discharges. Sampling took part at crucial moments of the flood that occurred thereafter: at first flushes (t17-t19-t23), before the flow peak (t32-t37), during the flow peak (t38-t41), following the release of water from the upstream Vinça reservoir (t44-t61) and during the return to basal level (t68-t86-t109). ProxyDyn1 corresponds to the dynamics of particulate organic carbon (/20 mg/l), which represented the dynamics of water flow, also represented in figure, total suspended solids, total organic carbon, total nitrogen, and terbuthylazine parameters. ProxyDyn2 corresponds to aminomethyl phosphonic acid (AMPA, µg/l), which represented glyphosate, phosphate, copper, temperature, *E. coli*, enterococci, diclofenac, sulfamethoxazole and carbamazepine parameters. ProxyDyn3 corresponds to lead (/150 µg/g) in the representation of the dynamics of cadmium, zinc, and conductivity parameters. ProxyDyn4 corresponds to pH (/70), which represented cobalt, nickel, and chrome parameters. Three parameters, Diuron, 2.4D and NO<sub>3</sub><sup>-</sup>, had a unique dynamic. For further details on statistical analyses for environmental parameters, see Noyer *et al.* (2020).

**Fig. 2** Alpha diversity of the archaeome of the Têt river along time. Changes in observed OTU number (blue) and Shannon index (red) along the flood (tX) and at summer and winter droughts (SD and WD respectively). For the Shannon index, different letters indicate a significant difference between samples (dunn.test<0.025) and red arrows show major significant differences. Observed OTU number was not significantly different (KW=0.14). The dotted profile is the flow level at each sampling point (see Fig. 1, also for sample names). Even though the absence of replicates for t61 and t68 samples impeded statistical testing, they are represented through time for comparison.

**Fig. 3** Composition of archaeal communities averaged across replicates. Histogram of relative abundances (a) of the six major phyla and (b) of the ten major classes. Samples are organized according to sampling time from left to right: summer drought (SD), autumn flood (sample names are followed by a number that indicates the sampling time in hours after the beginning of the flood at t<sub>0</sub>), and winter drought (WD). The dotted profile is the flow level at each sampling point (see Fig. 1 for further details).

**Fig. 4** Structure of archaeal communities averaged across replicates. (a) Principal Coordinate Analysis (PCoA) and (b) hierarchical clustering with Ward D2 linkage method using Weighted-Unifrac dissimilarity computed on OTU average abundance. Lines indicate ANOSIM significant groups. Sample names are followed by a number that indicates the sampling time in hours after t<sub>0</sub> (see Fig. 1 for details). Significant codes \*\* and \*\*\* indicate p-value < 0.01 and < 0.001, respectively.

**Fig. 5** Redundancy analysis (RDA) biplot with scaling by sites on the normalized matrix of OTUs with an abundance ≥ 0.05%. The model explained 66.32% of the variance (p<0.05). Significance for axes and environmental dynamics after permanova analyses are indicated, p-value significance codes: \*\*\*<0.001<\*\*<0.01<\*<0.05. Sample names are followed by a number that indicates the sampling time in hours after the beginning of the flood at t<sub>0</sub>. For further details on sample names and retained environmental variable dynamics, see Fig. 1b. Perpendicular grey lines represent the projection of the corresponding samples onto the corresponding dynamics and approximate the value of that sample along the variable (Legendre and Legendre 2012).

**Fig. 6** (a) Molecular ecological network of the unique module significantly positively correlated with environmental dynamics, particularly ProxyDyn2 and Diuron (see Fig. 1b for details and sample names). (b) Histogram of total reads of OTUs with positive module membership in function of samples along the flood. (c) Same for OTUs with negative module membership. Environmental dynamics are followed by module correlation value between parenthesis and the p-value significant code as follows: \*\*\*<0.001<\*\*<0.01<\*<0.05. OTUs are colored according to their phylum. The positive and negative connectivities between OTUs are indicated by blue and red lines, respectively. Only OTUs with a significantly correlated abundance profile with module are represented in this figure.

**Fig. 7** Summary of joined bacterial and archaeal network analysis. Each colored rectangle represents a module whose number appears at the bottom left corner of each rectangle together with the percentage of reads in the module out of the total number of reads analyzed within the network. The number of OTUs and the proportion of

reads within each module for each domain: archaea (A) and bacteria (B) are also indicated in each rectangle. At the top left of each rectangle the environmental dynamics are indicated with module eigengene correlation value between parentheses and the p-value significant code as follows: \*\*\*<0.001<\*\*<0.01<\*<0.05. The rectangle on the bottom right corner represents the six modules whose percentage of reads is less than 1% of the total number of reads analyzed in the network.

**Table 1** Summary of constraint-based multivariate statistical models on archaea OTU matrix averaged over replicates and without singletons. (a) Permanova significance of the five models tested and the percentage of biological variance that is explained by each model using permutation test with anova.cca function. (b) Axes and modeled variables significance after permanova using anova.cca of significant models in (a). p-values significance codes: (\*\*\*) < 0.001 < \*\* < 0.01 < \* < 0.05).

<b>a</b>	OTUs matrix transformation	Model significance	Variance (%)	
dbRDA	Jaccard	0.003**	63.38%	
	Unifrac	0.008**	66.35%	
	Bray-Curtis	0.326	60.04%	
	Weighted-Unifrac	0.004**	76.58%	
CCA		0.765	56.44%	
RDA	Hellinger	0.134	61.4%	

<b>b</b>	OTUs matrix transformation	Axes significance and variance explained (%)	Statistical significance of modeled variables						
			CAP1	ProxyDyn1	ProxyDyn2	ProxyDyn3	ProxyDyn4	2.4D	Diuron
dbRDA	Jaccard	0.002** (22.74)	0.001***	0.002**	0.001***	0.105	0.095	0.001***	0.096
	Unifrac	0.040* (30.24)	0.001***	0.021*	0.046*	0.458	0.383	0.036*	0.014*
	Weighted-Unifrac	0.006** (42.89)	0.006**	0.009**	0.039*	0.050*	0.004**	0.002**	0.166



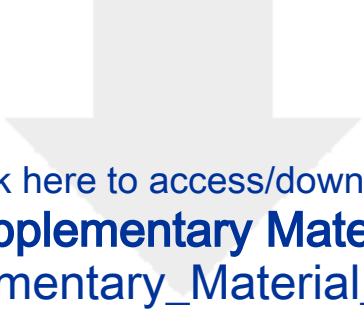
Click here to access/download  
**Supplementary Material**  
Supplementary\_Material\_S1.xlsx





Click here to access/download  
**Supplementary Material**  
Supplementary\_Material\_S3.xlsx





Click here to access/download  
**Supplementary Material**  
Supplementary\_Material\_S2.pdf



Click here to access/download  
**Supplementary Material**  
ReponseReviewersComments.pdf

